Sterically encumbered mixed sandwich compounds of uranium(III): synthesis and reactivity with small molecules

Rachel J. Kahan,[a] Joy H. Farnaby,*[ab] Nikolaos Tsoureas,[a] F. Geoffrey N. Cloke,[a] Peter B. Hitchcock,[a] Martyn P. Coles,[a] S. Mark Roe[a] and Claire Wilson[b]

[a]Department of Chemistry, School of Life Sciences, University of Sussex, Brighton, BN1 9QJ, United Kingdom

[b]School of Chemistry, WestCHEM, University of Glasgow, Glasgow G12 8QQ, United Kingdom

*Corresponding author: joy.farnaby@glasgow.ac.uk School of Chemistry, WestCHEM, University of Glasgow, Glasgow G12 8QQ, United Kingdom

Dedicated to Professor W. J. Evans on the occasion of his 70th birthday. Bill, you are an inspiration to us all.

Abstract

A series of uranium(III) mixed sandwich complexes with sterically demanding Cp^R ligands, of the type [U(COT^{TIPS2})(Cp^R)] (Cp^R = Cp^{tBu} ($C_5H_4{}^tBu$), Cp^{tBu2} ($C_5H_3{}^tBu_2$-1,3), Cp^{tBu3} ($C_5H_2{}^tBu_3$-1,2,4), Cp^{TIPS2} ($C_5H_3(Si^iPr_3)_2$-1,3), Cp^{Me4Bz} ($C_5Me_4CH_2Ph$), Ind^{Me6} (C_9HMe_6) and Ind^{Me7} (C_9Me_7), and COT^{TIPS2} = $C_8H_6(Si^iPr_3)_2$-1,4), have been synthesised and their X-ray crystal structures determined. The reactivity of these complexes with CO and CO_2 is reported, including the squarate complex [U(COT^{TIPS2})(Ind^{Me6})]$_2$(μ-C_4O_4), IR data on the long-lived carbonyl complex [U(COT^{TIPS2})(Ind^{Me7})(CO)] and the carbonate complex [U(COT^{TIPS2})(Cp^{tBu})]$_2$(μ-η^1:η^2-CO_3). The Solid-G algorithm has been to assess the steric properties of these and previously reported mixed-sandwich complexes in the solid state and correlate these properties with the observed reactivity.

1. Introduction

The molecular non-aqueous chemistry of uranium is a growing research area and in recent decades there have been many significant advances, including the preparation of new uranium-element multiple bonds, the isolation of new oxidation states and the reduction of the strongest bonds in nature by uranium(III) complexes.[1] It would be difficult to over-emphasise the importance of the supporting ligand environment in organo-actinide chemistry and even the most established organometallic ligand environments are still surprising us with new discoveries.[2] This is well-illustrated in the isolation of the first examples of uranium(II)[3] and plutonium(II)[4] in silylated tris-cyclopentadienyl ligand environments, [(2.2.2-cryptand)K][Cp′$_3$U] (′ = $SiMe_3$) and [(2.2.2-

cryptand)K][Cp′′$_3$Pu]. It is notable that changing the ligand environment can change the ground state electronic structure. The spectroscopic and theoretical data are consistent with a $5f^3 6d^1$ ground state in [(2.2.2-cryptand)K][Cp′$_3$U] but with a $5f^4$ ground state supported by δ back-bonding in [(2.2.2-cryptand)K][{(^{Ad,Me}OAr)$_3$mes}U], which is also formally uranium(II).[5]

Control of the ligand environment has also resulted in control of the reactivity of uranium(III) complexes, particularly in reductive transformations of N_2, CO and CO_2.[1b,6] There are a variety of complexes featuring different ligand classes that are competent for small molecule activation, and varying the substituents on these ligands has led to the synthesis of a range of novel fragments and unusual coordination modes, including a uranium(III)/uranium(IV) mixed valence bimetallic complex with a μ:η^1:η^1-CO bridge[7] and the only example of a terminally bound dinitrogen ligand on uranium, [Cp*$_3$U(η^1-N_2)].[8] Another powerful example is the isolation of both the first dinitrogen complex of uranium[9] and the first terminal uranium nitride[10] in the triamidoamine ligand environment; the parent uranium(III) complexes differ only in the substitution of the silyl R-groups. The Cloke group have reported extensive studies on the reductive activation of CO and CO_2 by uranium(III) mixed sandwich complexes, and have shown a variety of oxocarbon fragments can be obtained, simply by altering the substituents on the Cp and COT rings.[11,12,13] There is a correlation between the 'global' steric environment and reactivity with small molecules, but more importantly, the selectivity of oxocarbon formation is modulated by steric bulk of the Cp^R group. We also observed that altering the substituents on these ligands has little effect on the U^{IV}/U^{III} redox potential, but that altering the electronic properties of the complexes by replacing the Cp^R ligand with a heterocyclic or tris(pyrazolyl)borate alternative led to completely different reactivity.[14]

Here we report the synthesis of very bulky mixed-sandwich complexes of uranium(III) and their reactivity of with CO and CO_2. We have also used the Solid-G algorithm,[15] to assess the steric properties of these and previously reported mixed-sandwich complexes in the solid state and correlate these properties with the observed reactivity.

2. Results and discussion

2.1 Synthesis of Mixed Sandwich Complexes

The seven mixed sandwich complexes [U(COT^{TIPS2})(Cp^R)] (Cp^R = Cp^{tBu} (**1**), Cp^{tBu2} (**2**), Cp^{tBu3} (**3**), Cp^{TIPS2} (**4**), Cp^{Me4Bz} (**5**), Ind^{Me6} (**6**), Ind^{Me7} (**7**)) were prepared by sequential salt metathesis reaction of UI_3 with K[Cp^R] and K_2[COT^{TIPS2}] in good to moderate yields (Scheme 1). Syntheses of **1**, **2** and **4** – **7** were carried out in two steps to include the isolation of the [$UI_2(Cp^R)(THF)_n$] intermediate, in accordance with the synthesis of [U(COT^{TIPS2})(Cp*)(THF)].[11c] The synthesis of **3**, however, was

adapted to a 'one-pot' methodology due to poor solubility of $[UI_2(Cp^{tBu3})(THF)_n]$ in hydrocarbon solvents.[14a] Additionally, complexes **6** and **7** required cooling in the initial reaction step to prevent side reactions with the solvent.

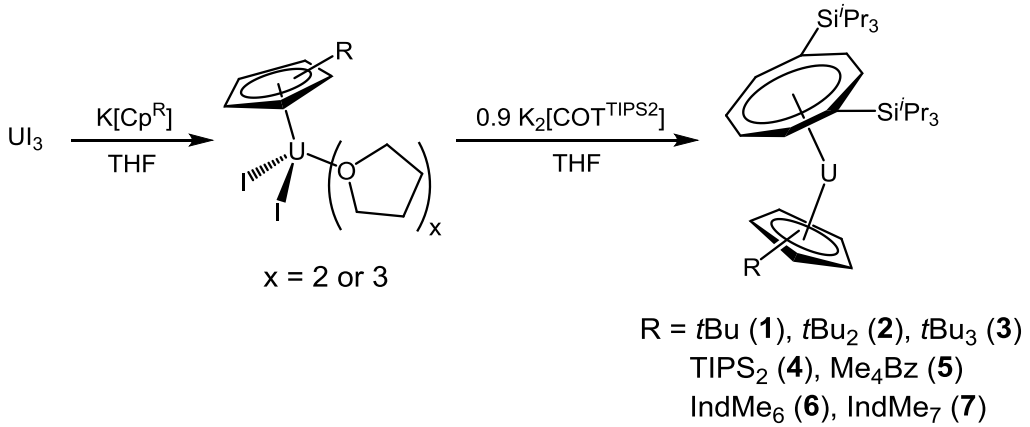

Scheme 1 Synthetic route to the uranium(III) mixed sandwich complexes **1** – **7**.

The seven mixed sandwich complexes display paramagnetically shifted ^{1}H and $^{29}Si\{^{1}H\}$ NMR resonances over a broad spectral window. In **1** – **3**, **5** and **7**, resonances could be assigned on the basis of relative integration and are consistent with free rotation and mirror plane symmetry on the NMR timescale. Complex **4** was shown to be fluxional at ambient temperature but could be resolved to illustrate a fully dynamic system with C_s symmetry above 35 °C, and a fixed system with C_1 symmetry below 5 °C. Complex **6** displayed a lower symmetry NMR spectrum at room temperature, which is consistent with the magnetic inequivalence of all ligand environments, and the Ind-C*H* resonance could not be identified, most likely as a result of broadening. Mass spectrometry and microanalysis support the formulation of **1** – **7**. Complex **1** was observed to form a stable adduct with THF (**1.THF**) in solution and the solid state but can be desolvated at room temperature without decomposition. This is in contrast to **2** – **7**, which are always isolated as base-free complexes because THF is readily removed under vacuum during work-up.

2.2 Structures of Mixed Sandwich Complexes

The solid-state molecular structures of **1** – **7** from single crystal X-ray diffraction studies are shown in Figures 1 – 3. The seven complexes are structurally analogous, and all adopt the bent configuration seen by other uranium mixed sandwich complexes.[11-14] The molecular structure of **1.THF** was also determined by single crystal X-ray diffraction (see Figure 1), and is directly comparable to $[U(COT^{TIPS2})(Cp^{Me4})(THF)]$ and $[U(COT^{TIPS2})(Cp^{*})(THF)]$.[11-12] The U–C and U–O distances within these complexes are similar, although **1.THF** exhibits the shortest U–O bond of the three, probably due to the ability of the *tert*-butyl substituent to be positioned away from

coordinated THF. There is also variation in the Ct1–U–Ct2 angle between the three complexes, attributed to interaction between the Cp substituents and the back of the COT ring. This angle is the smallest (i.e. deviates most from 180°) for **1.THF** as the *tert*-butyl substituent is positioned away from the COT ring in the orientation shown in Figure 1. Complex **1.THF** is also only the second complex in the uranium(III) mixed-sandwich series to be crystallised as both the THF-adduct and base-free complex (the other is [U(COT^{TIPS2})(Cp*)(THF)] and it is only desolvated upon heating at high vacuum) permitting comparison between the two solid state molecular structures. Lengthening of U–Ct1 and U–Ct2 is observed upon coordination of THF and the Ct1–U–Ct2 angle also decreases to accommodate the additional ligand. The same trend is also observed in the solid state molecular structures of [U(COT^{TIPS2})(Cp*)(THF)] and [U(COT^{TIPS2})(Cp*)], demonstrating the ability of the complex to flex upon addition of another ligand, in order to maintain an optimum steric environment.

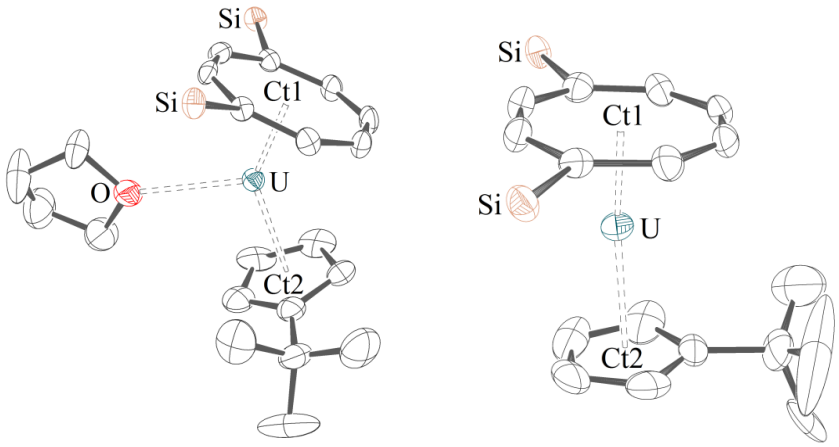

Figure 1 ORTEP diagram of **1.THF** and **1** (thermal ellipsoids at 50% probability; hydrogen atoms and ^{i}Pr groups have been omitted for clarity). Selected distances (Å) and angles (°) for **1.THF**: U–Ct1 1.9740(4) {1.9730(4)}, U–Ct2 2.5061(4) {2.5046(4)}, U–O 2.673(6) {2.671(6)}, Ct1–U–Ct2 140.574(19) {140.768(19)}. Numbers in brackets represent values from the second independent molecule in the asymmetric unit. Selected distances (Å) and angles (°) for **1**: U–Ct1 1.8891(7), U–Ct2 2.4950(7), Ct1–U–Ct2 174.66(4).

Complexes **1** – **3** exhibit lengthening of the U-Ct1 bond distance as the number of *tert*-butyl substituents increases, and an increase in tilt of the Cp ring (difference between the maximum and minimum values of U–C(Cp); 0.01 Å for **1**, 0.07 Å for **2** and 0.10 Å for **3**) in order to accommodate the extra steric bulk without increasing the average U–C distance (Figure 2). These observations further support the notion that the complexes flex to accommodate additional substituents in order to maintain an optimum steric environment. There is little difference in the metrics of **2** and **4**

despite the increased size of the TIPS group relative to the ^{t}Bu group. This is proposed to be due to the additional degrees of freedom associated with the *iso*-propyl groups, which allow them to be positioned away from the uranium atom. Complex **5** has the longest U–Ct1 bond of all the mixed sandwich complexes synthesised (although the U–Ct2 bond is of average length) and the smallest (most acute) Ct1–U–Ct2 angle. This is attributed to the position of the benzyl substituent, which sits perpendicular to and in-between the two TIPS substituents on the COT ring. This orientation is favourable as it minimises interaction between the benzyl fragment and the TIPS substituents and avoids interaction between the back of the COT ring with the benzyl substituent. It is of note that complexes **2** and **5** – **7** have two molecules in the asymmetric unit, which are packed and oriented to each other such that the uranium metal centres are very effectively encased and the U···U separation is minimised (Figures 2 and 3).

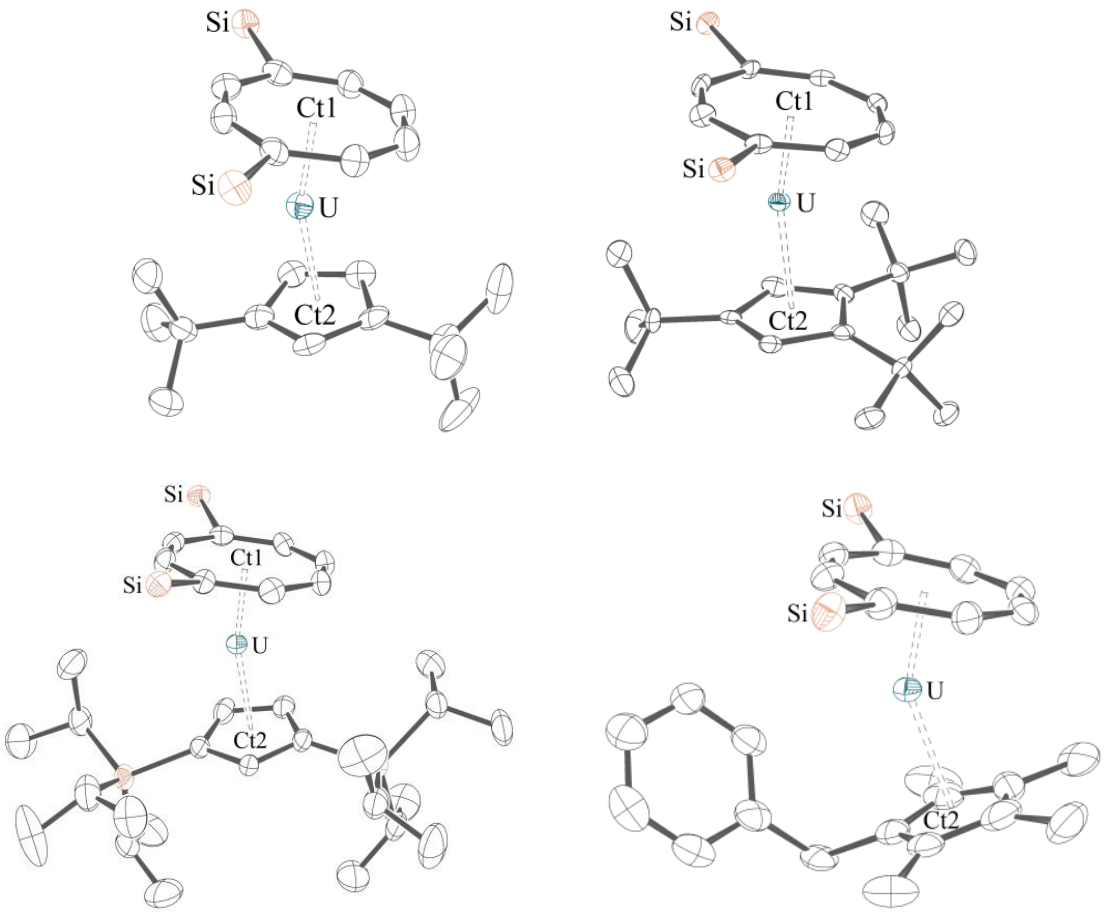

Figure 2 ORTEP diagram of **2** (top left), **3** (top right), **4** (bottom left) and **5** (bottom right). Thermal ellipsoids are depicted at 50% probability; hydrogen atoms and ^{i}Pr groups have been omitted for clarity. Selected distances (Å) and angles (°) for **2**: U–Ct1 1.9129(4) {1.9150(4)}, U–Ct2 2.4706(4) {2.4772(4)}, Ct1–U–Ct2 161.09(2) {159.83(2)}. Selected distances (Å) and angles (°) for **3**: U–Ct1 1.92263(18), U–Ct2 2.48047(18), Ct1–U–Ct2 167.042(10). Selected distances (Å) and angles (°)

for **4**: U–Ct1 1.9086(7), U–Ct2 2.4830(7), Ct1–U–Ct2 161.79(4). Selected distances (Å) and angles (°) for **5**: U–Ct1 1.942(2) {1.943(2)}, U–Ct2 2.477(3) {2.501(3)}, Ct1–U–Ct2 147.81(10) {155.41(11)}. Numbers in brackets represent values from the second independent molecule in the asymmetric unit.

Complexes **6** and **7** are isomorphous with η^5-coordination of the methylated indenyl ligand. They have very similar metrics to each other, which is also the case in the complexes they were designed to mimic, [U(COT^{TIPS2})(Cp*)(THF)] and [U(COT^{TIPS2})(Cp^{Me4H})(THF)] (Figure 3). Complexes **6** and **7** have comparable U–Ct1 distances to complexes **2** – **4** but display shorter U–Ct2 distances and Ct1–U–Ct2 angles that are comparable to the sterically encumbered complex **5**. The metrics can also be compared to the praseodymium analogue [Pr(η^5-Ind)(η^8-C_8H_8)$(THF)_2$], which features average Pr–C distances of 2.87 Å.[16] The range of U–C distances are also similar to those in the tris-indenyl complexes [U(η^5-Ind)$_3$] (2.7336(13) – 2.8463(10) Å), [U(η^5-Ind)$_3$Cl] (2.6716(4) – 2.8863(8) Å) and [U(η^5-$Ind^{1,4,7\text{-}Me3}$)$_3$Cl] (2.661(13) – 2.933(11) Å), demonstrating that there is little change in the distances upon addition of substituents to the indenyl ligand or changes in oxidation state between uranium(III) and uranium(IV).[17]

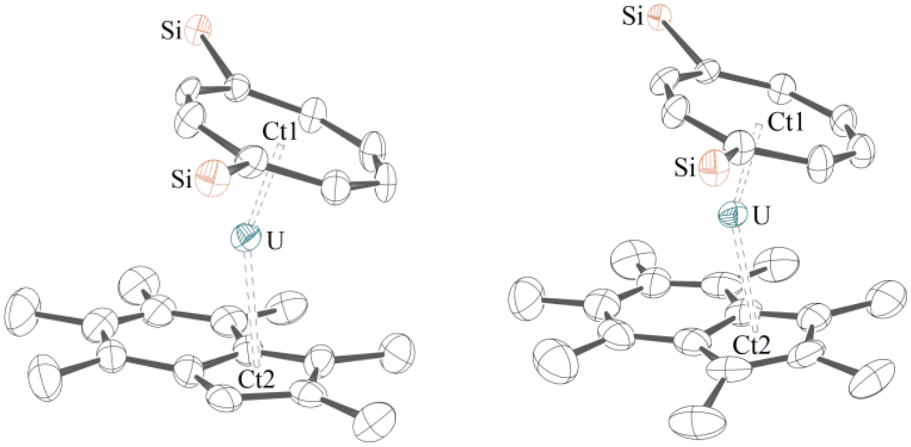

Figure 3 ORTEP diagram of **6** (left) and **7** (right). Thermal ellipsoids are depicted at 50% probability; hydrogen atoms and ^{i}Pr groups have been omitted for clarity. Selected distances (Å) and angles (°) for **6**: U–Ct1 1.907(3) {1.901(3)}, U–Ct2 2.459(4) {2.459(4)}, Ct1–U–Ct2 154.61(11) {153.90(11)}. Selected distances (Å) and angles (°) for **7**: U–Ct1 1.9177(18) {1.9057(15)}, U–Ct2 2.460(3) {2.4600(19)}, Ct1–U–Ct2 154.29(8) {152.27(7)}. Numbers in brackets represent values from the second independent molecule in the asymmetric unit.

2.3 Reactivity with CO

Complex **1** decomposes on addition of CO, regardless of the stoichiometry, to give no discernible products by ^{1}H NMR and only free ^{13}CO (δ 186 ppm) in the ^{13}C{^{1}H} NMR spectrum. However after several weeks in solution, crystals were obtained from the mixture, which were identified as the bridging oxo complex [U(COT^{TIPS2})(Cp^{tBu})]$_2$(μ-O) (**8**) (Scheme 2 and Figure 4). Complex **8**, can be independently synthesised by reaction of **1** or **1.THF** with N_2O, as confirmed by ^{1}H NMR of the isolated crystals. However, **8** was not observed by NMR in the reaction of **1** with CO within three weeks. It is therefore proposed that complex **8** is not one of the initial product of this reaction but forms later by reaction of one (or more) of the decomposition products.

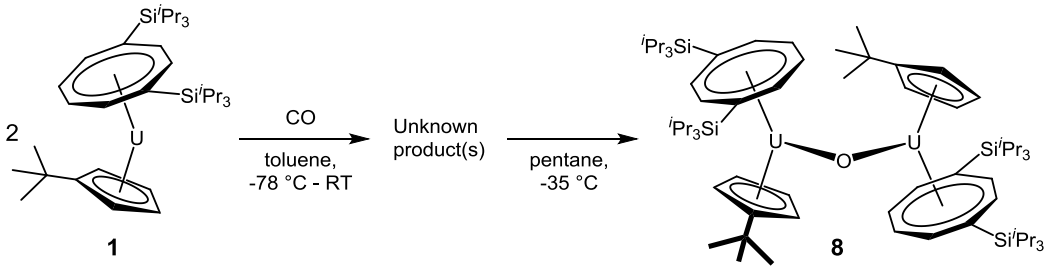

Scheme 2 Synthesis of [U(COT^{TIPS2})(Cp^{tBu})]$_2$(μ-O) (**8**).

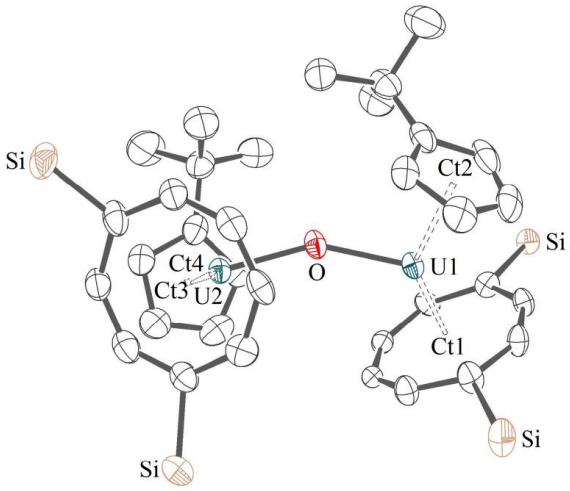

Figure 4 ORTEP diagram of **8** (thermal ellipsoids at 50% probability; hydrogen atoms and ^{i}Pr groups have been omitted for clarity). Selected distances (Å) and angles (°): U1–Ct1 1.9708(2), U2–Ct2 2.4932(2), U2–Ct3 1.9732(2), U2–Ct4 2.4959(2), Ct1–U1–Ct2 135.327(9), Ct3–U2–Ct4 136.724(10), U–O1 2.117(5), U–O1 2.110(4), Ct1–U1–U2–Ct3 108.549(2), Ct2–U1–U2–Ct4 136.2508(16).

Comparison of **8** with **1.THF** shows the Ct–U–Ct angle has decreased, but the U–COT and U–Cp distances are very similar to both **1** and **1.THF**. The COT rings are observed to have rotated so that the TIPS substituents are facing away from the oxo fragment and the U–O distances are comparable to other uranium(IV) mixed sandwich oxo complexes.[12b] The most striking aspect of the structure

of **8**, when compared to analogous complexes, is the twist and therefore large torsion angles between the two mixed-sandwich fragments. These are significantly larger than the corresponding torsion angles in $[U(COT^{TIPS2})(Cp^*)]_2(\mu\text{-}O)$ and $[U(COT^{TMS2})(Cp^*)]_2(\mu\text{-}O)$ (*ca*. 80 - 95°). We attribute this to the increased size and symmetrical shape of the Cp* ligand in comparison to Cp^{tBu}, and the acute angle in both Cp* analogues is proposed to arise in order to avoid unfavourable contacts between the ligands.

Complexes **2** – **5** demonstrate no reactivity with CO, even when subjected to 3 bar of the gas. The reaction of **6** with CO is exceptionally sensitive to reaction conditions. Although the conditions and stoichiometries were rigorously controlled (equivalents of ^{13}CO added *via* the Toepler line at - 78 °C), one main product but two different reaction outcomes were observed reproducibly by $^{13}C\{^1H\}$ NMR: either, no free ^{13}CO and two ^{13}C-labelled resonances were observed at δ 272.3 ppm and -63.5 ppm; or free ^{13}CO and only one resonance at δ -63.5 ppm were observed. Single crystals suitable for X-ray diffraction were grown from the reaction of **6** with 5 psi of CO and revealed the product at δ -63.5 ppm to be the squarate complex $[U(COT^{TIPS2})(Ind^{Me6})]_2(\mu\text{-}C_4O_4)$ (**9**) (Scheme 3). The negative chemical shift attributed to the squarate dianion at δ -63.5 ppm is comparable to the $^{13}C\{^1H\}$ NMR resonances of other uranium-bound squarate dianions, $[U(COT^{TIPS2})(Cp^{Me4})]_2(\mu\text{-}^{13}C_4O_4)]$ at δ -111.4 ppm and $[U(COT^{TMS2})(Cp^*)]_2(\mu\text{-}^{13}C_4O_4)$ at -127.1 ppm.[11-12] Further reactions to rationalise the mechanism or product distribution were unsuccessful, for example with a 50:50 mixture of $^{12/13}CO$ or CO/H_2. The functionalisation and removal of the squarate dianion was also not achieved. We cannot definitively assign the other ^{13}C-labelled product at δ 272.3 ppm to an oxocarbon, but it is most likely to be the uranium-bound deltate dianion, $[U(COT^{TIPS2})(Ind^{Me6})]_2(\mu\text{-}^{13}C_3O_3)]$. The $^{13}C\{^1H\}$ NMR resonance of $[U(COT^{TIPS2})(Cp^*)]_2(\mu\text{-}^{13}C_3O_3)$ at 225 ppm and the peak separation of 335 ppm between the deltate and squarate complexes is very similar to the 339 ppm difference between the deltate and squarate complexes of $[U(COT^{TIPS2})(Cp^*)]_2(\mu\text{-}^{13}C_3O_3)$ and $[U(COT^{TIPS2})(Cp^{Me4H})]_2(\mu\text{-}^{13}C_4O_4)$ (δ 225 and -111.4 ppm respectively).[11-12] We have never previously observed mixtures of squarate with other oxocarbons, but extreme sensitivity to reaction conditions (temperature, reaction time or shaking/stirring) has been previously noted during a study into the mechanism of the deltate formation.

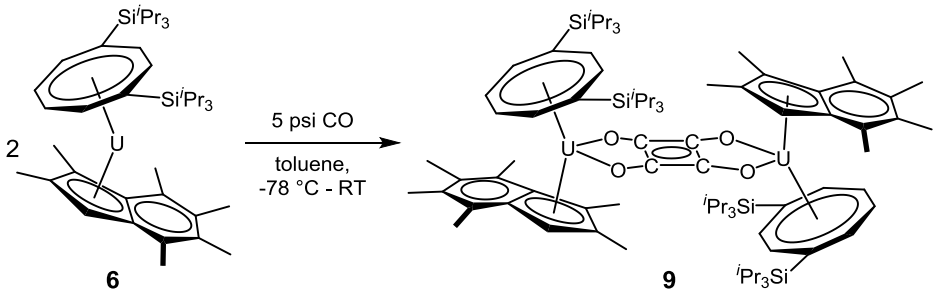

Scheme 3 Synthesis of $[U(COT^{TIPS2})(Ind^{Me6})]_2(\mu\text{-}C_4O_4)$ (**9**).

Unfortunately, full characterisation of **9** could not be achieved due to very poor yields; however single crystal X-ray diffraction supported the spectroscopic assignment of the complex (Figure 5). Comparison of the mixed sandwich fragment in **9** with **6** shows no significant lengthening of the uranium–ligand distances; however, the Ct1–U–Ct2 angle is smaller than the corresponding angle in **6**. The fold angle, which is defined as the deviation of the six-membered ring away from the plane of the five-membered ring, is also larger in **9** (6.6°) than in **6** and **7** (2.8 and 3.0° respectively) and the slip parameter has increased from -0.09 in **6** to 0.09 Å in **9**. Whilst this has no bearing on the hapticity of the indenyl ligand, it demonstrates the effects of increased steric crowding. The squarate unit is comparable to its analogue $[U(COT^{TIPS2})(Cp^{Me4})]_2(\mu\text{-}C_4O_4)$, which features the same U–O distances (2.477(5) and 2.471(6) Å) and marginally longer O1–C1 distances (1.272(9) and 1.269(10) Å) and C1–C1 distances (1.460(10) ad 1.499(10) Å).[11-12]

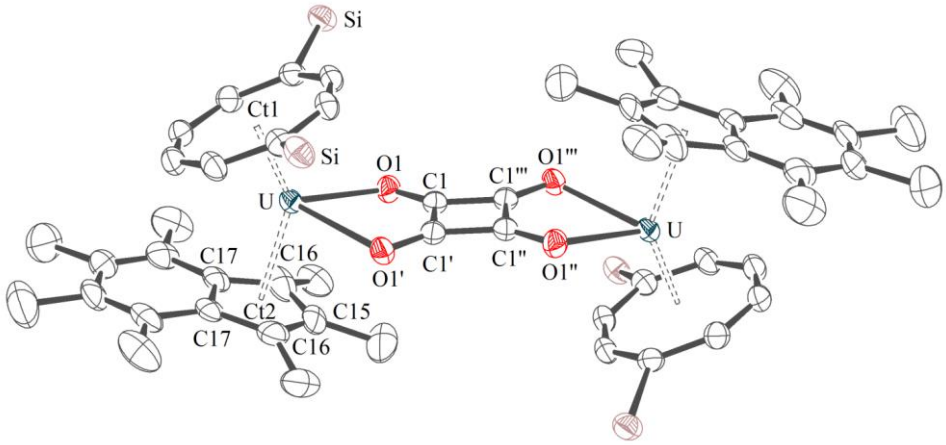

Figure 5 ORTEP diagram of **9** (thermal ellipsoids at 50% probability; hydrogen atoms and ^{i}Pr groups have been omitted for clarity). There is 50:50 Me/H occupancy at the C16 position. Selected distances (Å) and angles (°): U–Ct1 1.9475(5), U–Ct2 2.496(5), Ct1–U–Ct2 141.8(1), U–O1 2.472(3), O1–C1 1.259(5), C1–C1' 1.472(9), C1–C1" 1.442(9), C1–C1'–C1" 90.0, U–C15 2.758(5), U–C16 2.730(5), U–C17 2.820(5).

Complex **7** reacts immediately but reversibly with CO, which is lost on exposure to vacuum or if not maintained under a positive pressure of ^{13}CO, as adjudged by ^{1}H NMR and IR spectroscopy (Scheme 4). This species has a similar ^{1}H NMR spectrum to **7**, with significantly broadened resonances. No ^{13}C NMR resonances were observed when ^{13}CO was used. No uranium(III) carbonyl has been observed by $^{13}C\{^{1}H\}$ NMR but it is unusual not to observe free ^{13}CO. The reaction can be monitored by *in situ* React^{TM} IR spectroscopy in methylcyclohexane at -50 ºC, and displays a ν_{CO} of 1905 cm^{-1}. These data are consistent with the formation of the carbonyl complex

[U(COT^{TIPS2})(Ind^{Me7})(CO)] (**10**, Scheme 4). The reaction is best described as an equilibrium as when an excess of ^{12}CO was added to **10**, the ν_{CO} was observed to shift from 1905 cm^{-1} to 1945 cm^{-1}. Attempts to obtain single crystals from these reactions only yielded **7**, highlighting the reversibility of this reaction. Uranium(III) monocarbonyls[18] are found in the range 1880 – 1976 cm^{-1}, and are intermediates in the formation of oxocarbon complexes.[19] Complex **10** was seen to be long-lived as the ν_{CO} at 1905 cm^{-1} was observed after the reaction had been stirring for 12 hr at room temperature. This is in contrast to the only other example of a uranium(III) mixed sandwich monocarbonyl [U(COT^{TIPS2})(Cp*)(CO)], which is very short-lived (15 min). The ν_{CO} of **10** is only 15 cm^{-1} higher than the 1920 cm^{-1} in [U(COT^{TIPS2})(Cp*)(CO)].[19] However, the reduction in ν_{CO} from free CO does not correlate with the subsequent reactivity of the carbonyl species.

Exposure of a solution of **7** to ^{13}CO for 7 days results in conversion of **10** to another species with a ^{13}C{^{1}H} NMR resonance at δ 395 ppm. This is indicative of an oxocarbon complex, and is proposed to be the ynediolate complex, [U(COT^{TIPS2})(Ind^{Me7})]$_2$(μ-C$_2$O$_2$) (**11**).[20] The analogous ynediolate complexes [U(COT^{TIPS2})(Cp*)]$_2$(μ-C$_2$O$_2$), [U(COT^{TMS2})(Cp^{Me4Et})]$_2$(μ-C$_2$O$_2$) and [U(COT^{TMS2})(Cp^{Me4TMS})]$_2$(μ-C$_2$O$_2$) have ^{13}C resonances at δ 313, 315 and 287 ppm respectively.[11] Further addition of ^{13}CO to the reaction mixture after the formation of **11** did not result in a further reaction by ^{13}C{^{1}H} NMR, which is also consistent with ynediolate formation. The ^{1}H NMR spectrum of **11** is distinct from either **7** or **10** and the resonances associated with the COT^{TIPS2} ligand are consistent with a single Si^{i}Pr$_3$ environment rendered by mirror plane symmetry. However, the Ind-C*H*$_3$ are no longer symmetry equivalent, which is perhaps indicative of restricted rotation or a dimeric structure in solution. It is also of note that while four of the Ind-C*H*$_3$ resonances appear as sharp singlets, the other three are significantly broadened. However, in the absence of structural characterization, it would be premature to speculate about the hapticity of the indenyl ligand in **11**. No dimeric parent ion was observed by mass spectrometry of the crude reaction mixture and the only crystalline material isolated from the reaction was determined by X-ray crystallography to be **7**.

The NMR data for **10** and **11**, and the IR data of **10**, are directly analogous to the experimental observations in the reaction of [U(COT^{TIPS2})(Cp*)] with sub-stoichiometric ^{13}CO, which forms [U(COT^{TIPS2})(Cp*)]$_2$(μ-C$_2$O$_2$) only when it cannot react with more than one equivalent of CO.[19] The reactivity of both **6** and **7** with CO would appear to be thermodynamically similar to the [U(COT^{TIPS2})(Cp^{R})] complexes but under different kinetic control.

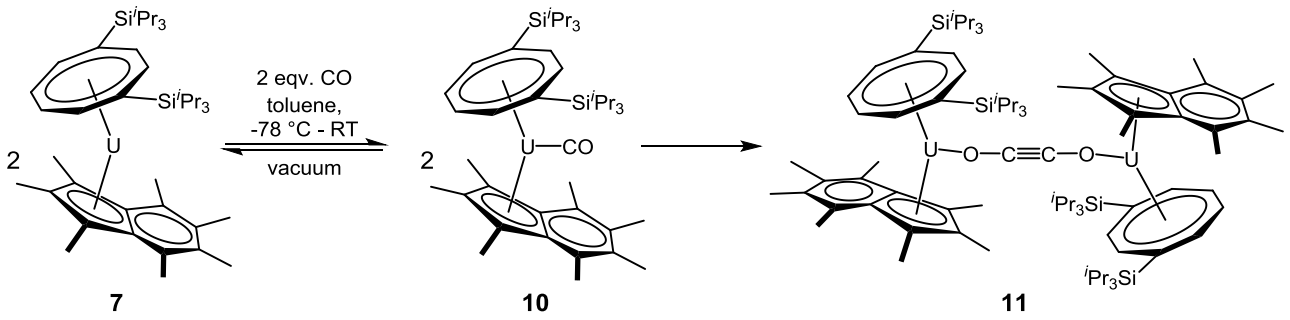

Scheme 4 Proposed reactivity of [U(COT^{TIPS2})(Ind^{Me7})] **7** with CO.

2.4 Reactivity with CO_2

Addition of excess CO_2 to complex **1** results in the formation of the carbonate complex [U(COT^{TIPS2})(Cp^{tBu})]$_2$(μ-η^1:η^2-CO_3) (**12**), which was confirmed by mass spectrometry, microanalysis and single crystal X-ray diffraction (Scheme 5 and Figure 6). The reaction can be monitored by ^{13}C NMR using $^{13}CO_2$, and shows the formation of **12** by the appearance of a broad resonance at δ 195.4 ppm ($w_{½}$ = 375 Hz), and free ^{13}CO at δ 185.4 ppm. The broad half-height linewidth of the carbonate carbon is suggestive of a fluxional bonding mode; however despite narrowing of the linewidth at cold temperatures, it was not possible to freeze out the fluxionality or obtain an averaged environment at higher temperatures. Using substoichiometric amounts of CO_2 also yielded **12** but the reaction did not reach completion.

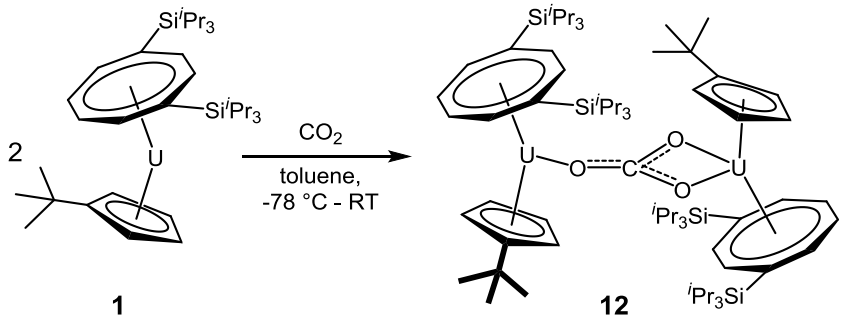

Scheme 5 Synthesis of [U(COT^{TIPS2})(Cp^{tBu})]$_2$(μ-η^1:η^2-CO_3) (**12**)

Single crystal X-ray diffraction of **12** shows μ-η^1:η^2-bonding of the carbonate unit, which is analogous to the other mixed-sandwich complexes, [U(COT^{TIPS2})(Cp*)]$_2$(μ-η^1:η^2-CO_3), [U(COT^{TIPS2})(Cp^{Me4H})]$_2$(μ-η^1:η^2-CO_3) and [U(COT^{TMS2})(Cp^{Me4R})]$_2$(μ-η^1:η^2-CO_3) (R = Et, *i*Pr, *t*Bu).[12] However **12** differs in that the Ct–U–U–Ct dihedral angles are non-linear, giving rise to a perpendicular twist between the two mixed-sandwich fragments (as also seen in **8**). This feature is assigned to the asymmetrical shape of the Cp^{tBu} ligand, which prevents unfavourable contacts

between the substituent atoms, whilst maintaining similar U–Ct1 and U–Ct2 distances and Ct–U–Ct angles within the mixed-sandwich unit.

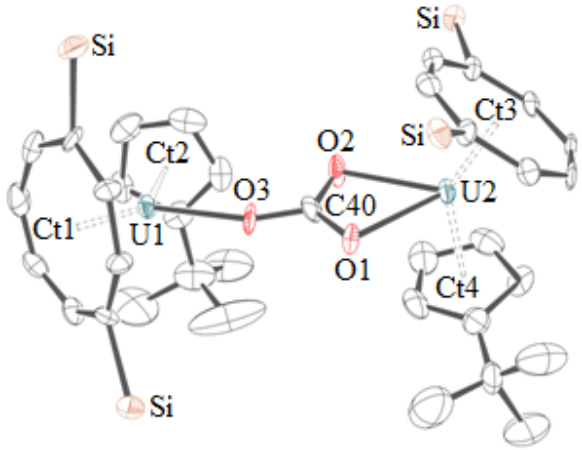

Figure 6 ORTEP diagram of **12** (thermal ellipsoids at 50% probability; hydrogen atoms and ^{i}Pr groups have been omitted for clarity). Selected distances (Å) and angles (°): U1–Ct1 1.9071(5), U1–Ct2 2.4651(5), U2–Ct3 1.9627(5), U2–Ct4 2.5021(5), Ct1–U1–Ct2 136.55(2), Ct3–U2–Ct4 136.85(2), Ct1–U1–U2–Ct3 77.6564(6), Ct2–U1–U2–Ct4 71.4376(5).

Complexes **3** and **4** react with CO_2 to yield a single product quantitatively by NMR (Scheme 6). However, the only resonance observed by ^{13}C NMR corresponded to free ^{13}CO. It is hypothesised that the complexes formed from these reactions are the dimeric bridging oxo complexes [U(COT^{TIPS2})(Cp^{R})]$_2$(μ-O) (**13** and **14**), however full characterisation of these species could not be achieved. This formulation is supported by the fact that the reactions of **3** and **4** with N_2O result in the same products by ^{1}H NMR. **2** and **5** are also believed to form [U(COT^{TIPS2})(Cp^{tBu2})]$_2$(μ-O) with CO_2, evidenced by a single resonance in the ^{13}C NMR spectrum corresponding to free ^{13}CO. However, a mixture of products was observed by ^{1}H NMR which could not be separated precluding further characterisation.

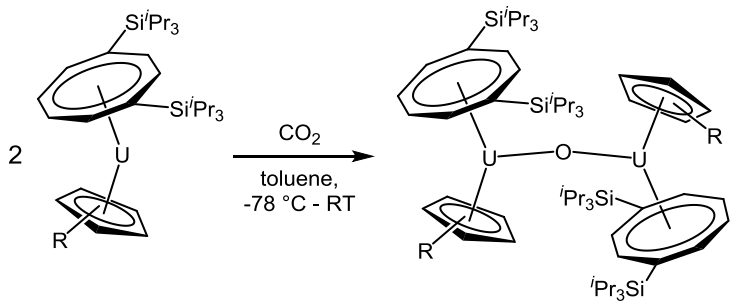

R = *t*Bu3 (**3**), TIPS2 (**4**) R = *t*Bu3 (**13**), TIPS2 (**14**)

Scheme 6 Proposed reactivity of [U(COT^{TIPS2})(Cp^{R})] with CO_2.

Complex **6** reacts with $^{13}CO_2$ under analogous conditions to the CO reactions, with a colour change from red/brown to bright red and the appearance of three product resonances in the $^{13}C\{^1H\}$ NMR in addition to resonances at δ 185 and 123 ppm for free ^{13}CO and free $^{13}CO_2$ respectively. Two of the ^{13}C-labelled products appear very close together at δ 210.5 and 209.2 ppm and the third resonance is a broad multiplet centered at δ -63.5 ppm, corresponding to **9**. These experimental observations are consistent with the reductive disproportionation of carbon dioxide to give the carbonate complex $[U(COT^{TIPS2})(Ind^{Me6})]_2(\mu\text{-}CO_3)$ (**15**) (Scheme 7), with concomitant formation of **9** from the competing reaction of **6** with CO. This reactivity has also been seen in for the other uranium(III) mixed sandwich complexes that are selective for the squarate dianion.[12] The two ^{13}C environments of δ 210.5 and 209.2 ppm, could be consistent with two different modes of coordination, such as $(\mu\text{-}\eta^1\text{:}\eta^2\text{-}CO_3)$ and $(\mu\text{-}\eta^2\text{:}\eta^2\text{-}CO_3)$ but more likely result from the asymmetry of the Ind^{Me6} ligand (there is 50/50 H/Me disorder in the occupancy of C16 position in **9**, see Figure 5) .

The reactivity of **7** with $^{13}CO_2$ was also accompanied by the same colour change and the appearance of a single resonance in the $^{13}C\{^1H\}$ NMR spectrum at δ 180.8 ppm, in addition to resonances at δ 184.8 and 123 ppm for free ^{13}CO and free $^{13}CO_2$ respectively. The experimental observation of free ^{13}CO and a single ^{13}C-labelled product suggest that **7** shares a similar reactivity with $^{13}CO_2$ to **6**, and forms the carbonate complex $[U(COT^{TIPS2})(Ind^{Me7})]_2(\mu\text{-}CO_3)$ (**16**). An excess of $^{13}CO_2$ in the $^{13}C\{^1H\}$ NMR spectrum is in also keeping with carbonate formation as the reaction to form a U(IV)-CO_3^{2-}-U(IV) species and ^{13}CO is stoichiometric. In spite of the clean reactions by NMR to form complexes **15** and **16**, no crystalline or microcrystalline material suitable for further characterization or X-ray diffraction studies could be obtained.

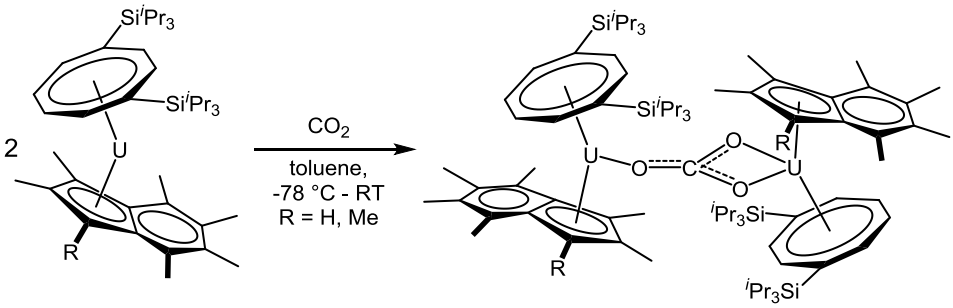

R = H (**6**), Me (**7**) R = H (**15**), Me (1**6**)

Scheme 7 Proposed reactivity of $[U(COT^{TIPS2})(Ind^R)]$ with CO_2.

2.5 Evaluation of the Steric Properties Using the Solid-G Algorithm

The clear influence of ligand design and environment on the properties and reactivity of uranium complexes has been demonstrated repeatedly in the literature. The use of density functional theory to evaluate the steric properties of complexes is both time consuming and computationally expensive, particularly for actinides, and the properties of molecules calculated in the gas phase do not always correlate with those obtained from experiment.[21] An alternative approach uses algorithms including Solid-G,[15] which calculates the shielding of the metal centre (the G-parameter) from the atomic coordinates obtained from single crystal X-ray diffraction data or molecular mechanics. Solid-G has been used successfully for comparing the steric properties of differing ligands in both transition metal and lanthanide complexes and has proved effective in rationalising differences in structure and reactivity.[22] We have used the Solid-G algorithm to evaluate the steric parameters of **1**–**7** and previously published uranium(III) mixed sandwich complexes from X-ray diffraction data, thereby allowing comparison of the ligand contribution and overall shielding in the solid state. This algorithm was of particular interest to us because it allows very rapid (less than 10 seconds) calculation of the steric properties of the complexes.

Comparison of the G-parameter for the Cp^R ligands illustrates that as the number and size of the substituents increases, the shielding of the uranium centre by the Cp^R ligand increases from 28 – 40% (see Figure 7, green). This is a significant change and, given the COT^{TIPS2} ligand has a G-parameter in the range of 48.4 to 54.1% (Figure 7, blue), clearly illustrates that the coordination sphere is fully saturated when coordinating the larger ligands. The variation in U-Cp/U-COT distances and the degrees of freedom exhibited by the substituents contribute significantly to the calculated G-parameters. This is best observed for the COT^{TIPS2} G-parameter where a good correlation was found between the Ct1–C–Si angle and the COT^{TIPS2} G-parameter (see Figure 8). This trend clearly accounts for the variation in the COT^{TIPS2} G-parameter, but cannot be determined with any degree of accuracy for the Cp^R ligand due to the varying number and nature of the substituents.

A similar study on substituent effect on the activation of CO_2 by $Ttz^{R,R}$ complexes of zinc found a more significant variation in the G-parameter (55 - 72%) when altering the R substituents, although for $Ttz^{Ph,Me}$ the value was observed to be less than expected due to twisting of the phenyl ring which allows greater flexibility and the formation of more crowded complexes.[22a] Clearly the flexibility and degrees of freedom present in the COT^{TIPS2} ligand has a similar effect, as G_{SUM} only varies by 9% (see Table 1). It is also believed that this ability to flex accounts for some inconsistencies in the order of ligand size. For example, [U(COT^{TIPS2})(Cp^{Me4Et})] has a smaller G_{SUM} than both [U(COT^{TIPS2})(Cp*)] and [U(COT^{TIPS2})(Cp^{tBu})] (see Table 1), but also has smaller (i.e. deviates most from 180°) Ct1–C–Si angles than the other two complexes (see Figure 8).

Calculation of the G-parameter has also highlighted that there is an optimum steric environment for the mixed sandwich complexes, as has been demonstrated by the work of Fukin *et al.*.[23] In this instance, the optimum environment is maintained by coordination of THF for the smaller complexes and an increased bending of the TIPS substituents away from the metal centre and substituent meshing for the larger complexes. The latter two points are highlighted by [U(COT^{TIPS2})(Cp^{Me4Bz})], which not only has smaller Ct1–C–Si angles (168.2(4) and 173.6(4)°) but also exhibits a higher degree of meshing, accounting for loss of 0.29 and 0.34% shielding for each independent molecule in the asymmetric unit (see Figure 7). In comparison, [U(COT^{TIPS2})(Cp^{tBu})], which has the smallest Cp^{R} G-parameter, has the most linear Ct1–C–Si angles (177.38(6)°) and no meshing at all. The values for U(COT^{TIPS2})(Cp^{tBu})] and [U(COT^{TIPS2})(Cp*)], which are the only two complexes that can be crystallised with and without coordinated THF, also demonstrate the importance of flexibility, as whilst the G-parameters for THF are in the range of 10 - 13%, G_{SUM} only increases by 6% upon THF coordination.

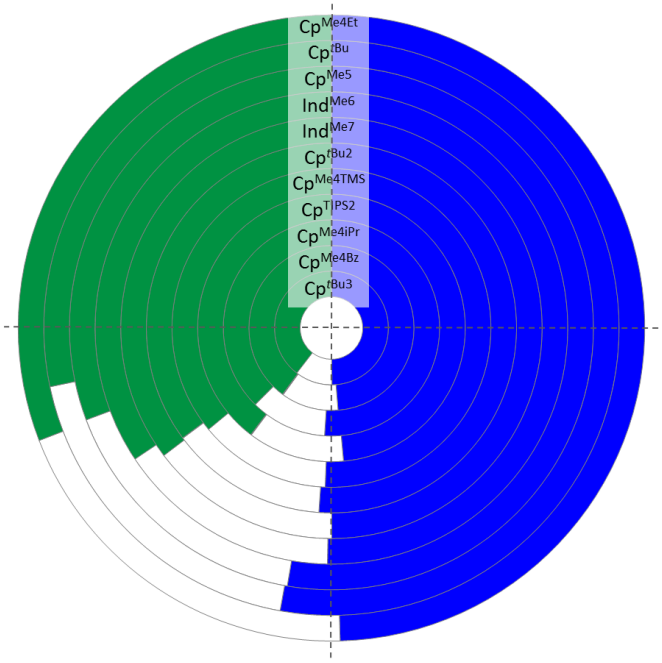

Figure 7 The G parameter for the COT^{TIPS2} ligand (blue), the Cp^{R} ligand (green) and the non-shielded area of the uranium atom (white). Areas of overlap between the COT^{TIPS2} and Cp^{R} ligand (Gγ) are shown in dark blue between the blue and white data. Complexes are shown in ascending order of G_{SUM} from the outside to the centre. Where there is more than one molecule in the asymmetric unit the average G_{SUM} is shown.

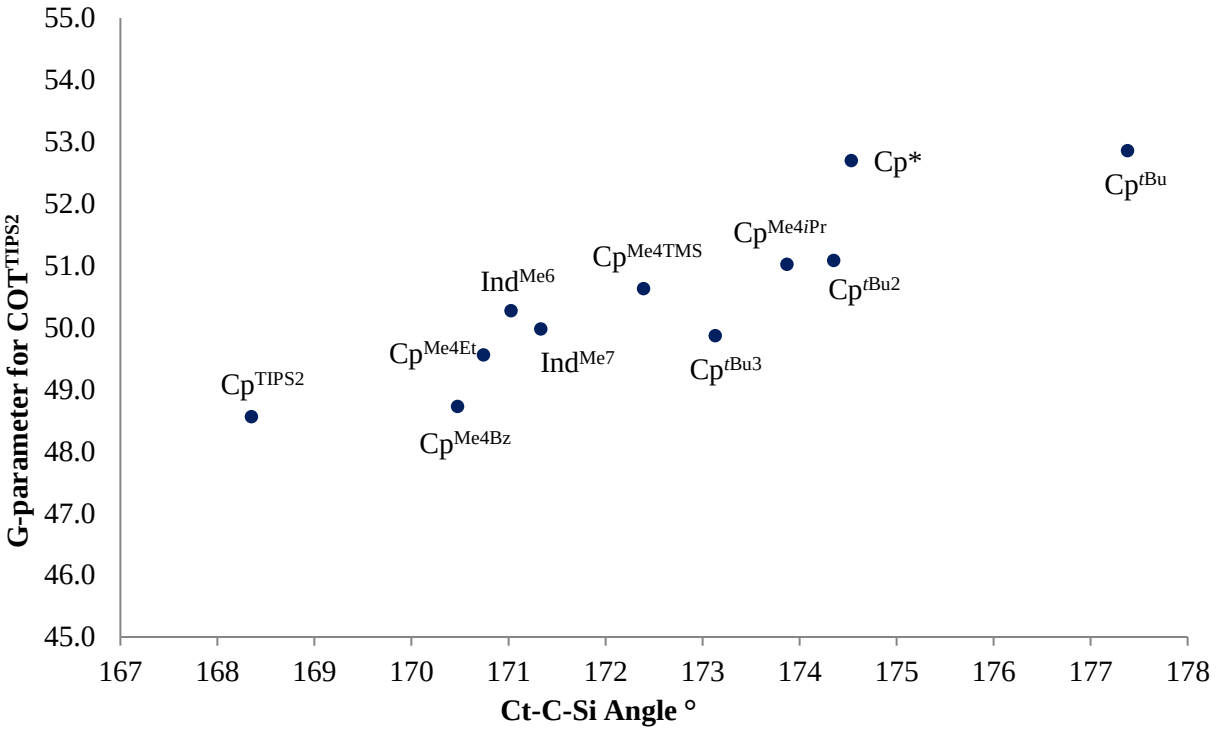

Figure 8 The influence of the Ct1–C–Si angle on the COT^{TIPS2} G-parameter for a series of uranium(III) mixed sandwich complexes [$U(COT^{TIPS2})(Cp^{R})$].

Comparing the G_{SUM} values with the observed CO reactivity illustrates that any base-free complex which exhibits more than 86% shielding (in the absence of THF) does not react with CO under the conditions studied (up to 3 bar CO, up to 110 °C). Similarly, base free complexes with G_{SUM} of 86% or greater only give rise to oxo complexes or unidentified mixtures upon reaction with CO_2 (see Table 1). The fact that **6** and **7** show similar reactivity to cyclopentadienyl complexes featuring less shielding, demonstrates the shape of the ligand is just as important, if not more so, than its size. It was also observed that complexes only react with CO when there is a significantly sized void at the front of the complex between the two TIPS substituents (see Figure 9). For the complexes with coordinated THF, the solvent molecule occupies the void, but is sufficiently labile to allow coordination of the reactive molecule under the conditions studied (see Figure 10). For the base-free complexes this void appears substantial and, based on the available data the reactivity pocket, appears to comprise of 5 – 10% of the surface of the sphere when the G-parameters of the other ligands (including THF) are taken into account.

Table 1 Comparison of the G-parameter with the observed reactivity for [U(COT^{TIPS2})(Cp^{R})] complexes. Values in italics represent those obtained from [U(COT^{TIPS2})(Cp^{R})(THF)] complexes.

R	$G_{complex}$	G_{CpR}	Outcome with CO[11]	Outcome with CO_2[12]
Me_4Et	80.41	30.85	ynediolate and deltate[c]	unidentified mixture
^{t}Bu	81.14 *87.82*[a]	28.28 *28.11*[a]	decomposition	carbonate
Me_4	*88.56*	*28.56*	squarate[b]	carbonate
Me_5	83.42[a] *89.30*	30.71[a] *29.81*	deltate[a]	carbonate
Ind^{Me6}	84.64	34.86	squarate or mixture of products	carbonate[c]
Ind^{Me7}	85.34	35.36	carbonyl and ynediolate[c]	carbonate[c]
$^{t}Bu_2$	86.22[a]	35.14[a]	no reaction	unidentified mixture
Me_4SiMe_3	86.61	35.98	no reaction	oxo
$(Si^{i}Pr_3)_2$	88.26	39.73	no reaction	oxo[c]
Me_4Bz	88.44[a]	39.96[a]	no reaction	unidentified mixture
$Me_4{}^{i}Pr$	88.56	37.54	no reaction	oxo
$^{t}Bu_3$	89.44	39.56	no reaction	oxo[c]

[a]Average of values where there is more than one molecule in the asymmetric unit. [b]Present as a mixture. [c]Proposed product.

It should be stressed that whilst the values generated by Solid-G provide a means of quantitatively comparing the steric properties of the mixed sandwich complexes in the solid-state molecular structures, they cannot be used to accurately predict the behaviour of the complexes in solution, and therefore suffer a similar drawback to DFT. In addition, this method cannot account for changes in the electronic properties of the complex, which have been found to contribute significantly to small

molecule reactivity.[14] We therefore suggest that this method is most useful for understanding the solid state molecular structures of a series of complexes and evaluating the flexibility of ligands. Using the latter, we can establish the suitability of a ligand when designing complexes which require structural change or rearrangement in order for a reaction to take place and to approximate the size and shape of a reactivity pocket.

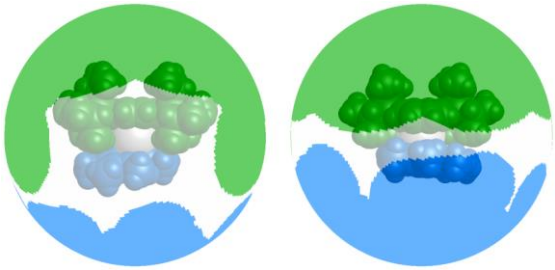

Figure 9. Visualisation of the front (left) and back (right) of the coordination sphere of **7**. COT^{TIPS2} and its shadow on the surface of the sphere is shown in green and Ind^{Me7} and its shadow on the surface of the sphere is shown in blue. White areas on the sphere's surface represent the accessible surface of the uranium centre.

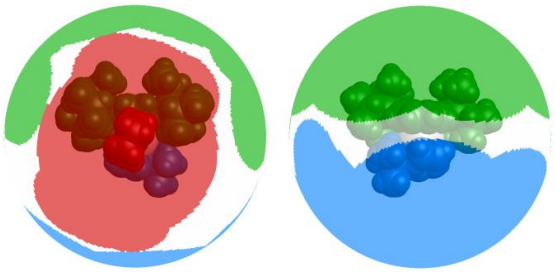

Figure 10. Visualisation of the front (left) and back (right) of the coordination sphere of **1.THF**. The coordinated THF molecule and its shadow on the surface of the sphere is shown in red, the COT^{TIPS2} and its shadow on the surface of the sphere is shown in green, and Cp^{tBu} and its shadow on the surface of the sphere is shown in blue. White areas on the sphere's surface represent the accessible surface of the uranium centre.

3. Concluding remarks

The seven mixed sandwich complexes $[U(COT^{TIPS2})(Cp^{R})]$ (Cp^{R} = Cp^{tBu} (**1**), Cp^{tBu2} (**2**), Cp^{tBu3} (**3**), Cp^{TIPS2} (**4**), Cp^{Me4Bz} (**5**), Ind^{Me6} (**6**), Ind^{Me7} (**7**) have been synthesised and their X-ray crystal structures determined. With the exception of **1**, which can be isolated with or without coordinating THF (**1.THF** and **1** respectively), the solid state molecular structures of complexes **2** – **7** are base-free. Complex **1** decomposes with CO but reacts with CO_2 *via* reductive disproportionation to form the carbonate complex $[U(COT^{TIPS2})(Cp^{tBu})]_2(\mu\text{-}\eta^1\text{:}\eta^2\text{-}CO_3)$ (**12**). The most sterically encumbered

complexes, **2** – **4** display no reactivity towards CO, which we attribute to the high entropic cost of CO binding in these complexes. Complexes **2** – **4** do react with CO_2 but form $[U(COT^{TIPS2})(Cp^R)]_2(\mu\text{-}O)$, with some decomposition. Complex **6** reacts with CO to form two oxocarbon products, one of which is the squarate complex $[U(COT^{TIPS2})(Ind^{Me6})]_2(\mu\text{-}C_4O_4)$ (**9**). Complex **7** reacts with CO reversibly to form a long-lived carbonyl complex $[U(COT^{TIPS2})(Ind^{Me7})(CO)]$ (**10**) and then subsequently to a single oxocarbon product. Complexes **6** and **7** react with CO_2 *via* reductive disproportionation to form carbonate complexes and in the case of **6**, concomitant formation of complex **9** is observed from the CO liberated by the reaction. The reactivity of both **6** and **7** with small molecules would appear to be thermodynamically similar to the $[U(COT^{TIPS2})(Cp^R)]$ complexes, but under different kinetic control. The values of G_{SUM} calculated using the Solid-G algorithm clearly illustrates that the coordination sphere is saturated in these very bulky complexes. The variation in U–Cp/U–COT distances and the degrees of freedom exhibited by the substituents contribute significantly to the calculated G-parameters and a good correlation was found between the Ct1–C–Si angle and the COT^{TIPS2} G-parameter. It was observed that complexes will only react with CO when there is a significantly sized void for reactivity, comprising of 5-10% of the coordination sphere. The fact that **6** and **7** show similar reactivity to cyclopentadienyl complexes featuring less shielding, demonstrates the shape of the ligand is just as important, if not more so, than its size.

4. Experimental Section

4.1 General Considerations

All manipulations were carried out in an MBraun glovebox under N_2 or Ar (O_2 and H_2O <1 ppm) or by using standard Schlenk techniques under Ar (BOC Pureshield) passed through a column containing BASF R3-11(G) catalyst and activated molecular sieves (4 Å). Solvents were dried over appropriate drying agents (NaK_3, pentane, hexane, diethyl ether; K, toluene, THF) prior to distillation under N_2. Solvents were stored over K mirrors or 4 Å molecular sieves. Deuterated solvents were dried over K, vacuum distilled and stored over 4 Å molecular sieves under Ar. NMR spectra were recorded on a Varian VNMR spectrometer operating at 400 MHz (^{1}H), 100 MHz (^{13}C) and 79 MHz (^{29}Si). ^{1}H and ^{13}C spectra were referenced internally to residual solvent signals and ^{29}Si spectra were referenced externally to $SiMe_4$. NMR spectra were recorded at 303 K unless otherwise stated. EI-MS was performed by Dr A. K. Abdul-Sada at the University of Sussex using a VG Autospec Fisons instrument. Elemental analyses were performed by Mikroanalytisches Labor Pascher or the University of Bristol Microanalysis Service. The following materials were purchased

from Aldrich and used as received: tri-*iso*-propylsilyltriflate, 2,3,4,5-tetramethyl-2-cyclopentenone, p-toluenesulfonic acid, NaH and KH. Solutions of $PhCH_2MgCl$ (0.1 M in THF) was purchased from Alfa-Aesar and used as received. $K[N(SiMe_3)_2)]$ was purchased from Aldrich and recrystallised from toluene prior to use. Dicyclopentadiene was purchased from Aldrich and cracked according to published procedures.[24] Solutions of ^{n}BuLi (*ca*. 2.5 M in hexanes) were supplied by Acros Organics and titrated to determine the exact molarity prior to use. $KInd^{Me6}$, was donated by Prof. F. G. N. Cloke and $HInd^{Me7}$ by Prof. D. O'Hare, Oxford University. $HInd^{Me7}$ was deprotonated using $K[N(SiMe_3)_2)]$ in toluene. The following materials were prepared according to published procedures: UI_3,[25] $H[Cp^{tBu}]$,[26] $H[Cp^{tBu2}]$,[26] $H[Cp^{tBu3}]$,[26] $K[CH_2Ph]$,[27] and $K_2[C_8H_6(Si^{i}Pr_3)_2\text{-}1,4]$ (referred to as $K_2[COT^{TIPS2}]$).[28] Gases: ^{13}CO (99.7% enrichment) was purchased from EuroIsotop, $^{13}CO_2$ (99%) from Cambridge Isotopes and N_2O (purity >99.998%) from Fluka. Labelled gases were transferred *via* a calibrated Toepler pump. Na[Cp], $K[Cp^{tBu}]$, $K[Cp^{tBu2}]$ and $K[Cp^{tBu3}]$ were prepared by deprotonation of the neutral ligands with NaH or KH in THF/toluene.[29]

4.2 $K[Cp^{TIPS2}]$

To a solution of Na[Cp] (3.126 g, 36.5 mmol) in THF (50 mL) at -78 °C was added a solution of tri-*iso*-propylsilyltriflate (11.175 g, 36.4 mmol) in hexane (30 mL) dropwise over 1 hour. The crude Cp^{TIPS} was warmed to ambient temperature then dried *in vacuo* and extracted in hexane (150 mL) to give a yellow solution. To this was added dropwise a solution of ^{n}BuLi (14.3 mL, 35.7 mmol) over 1 hour at -10 °C. The mixture was warmed to ambient temperature and stirred for 12 hours then all volatiles were removed *in vacuo* to give $Li[Cp^{TIPS}]$ as an off-white solid (8.20 g, 35.9 mmol). $Li[Cp^{TIPS}]$ was dissolved diethyl ether (100 mL) and a solution of tri-*iso*-propylsilyltriflate (10.944 g, 35.7 mmol) in hexane (30 mL) was added dropwise at -78 °C over 1 hour. The mixture was warmed to ambient temperature and stirred for 12 hours then all volatiles were removed *in vacuo*. Cp^{TIPS2} was extracted in hexane (200 mL) and filtered then the solvent volume was reduced to 30 mL. To this was added a solution of $K[N(SiMe_3)_2)]$ (6.898 g, 34.6 mmol) in toluene (20 mL) dropwise at ambient temperature. The mixture was stirred for 3 hours then filtered to give an orange/brown solution from which beige solids were obtained *in vacuo* (12.69 g, 83%). ^{1}H NMR (C_7D_5N): δ 6.9 (m, 1H, Cp-*H*), 6.8 (m, 2H, Cp-*H*), 1.4 (m, 6H, ^{i}Pr-C*H*), 1.3 (d, 36H, $^3J_{HH}$ = 7.27 Hz, ^{i}Pr-CH_3,). $^{13}C\{^1H\}$ NMR (C_7D_5N): δ 126.6 (Cp-C2), 117.9 (Cp-C4, Cp-C5), 107.9 (Cp-C1, Cp-C3), 20.6 (^{i}Pr-*C*H_3), 13.5 (^{i}Pr-*C*H,). $^{29}Si\{^1H\}$ NMR (C_7D_5N): δ -4.1 ($Si^{i}Pr_3$).

4.3 K[Cp^{Me4Bz}]

A 3 neck 250 ml round bottomed flask equipped with condenser, pressure equalising dropping funnel and an inert atmosphere inlet adapter was charged with $PhCH_2MgCl$ in THF (100 mL, 100 mmol), THF (20 mL) and diethyl ether (100 mL) and cooled to 0 °C. To this was added 2,3,4,5-tetramethyl-2-cyclopentenone (10 g, 72 mmol, previously degassed) *via* the dropping funnel over 90 minutes. The reaction mixture was slowly warmed to room temperature and stirred for 12 hours. The resulting yellow solution was cooled at 0 ºC and quenched with MeOH (ca 10 mL) *via* the dropping funnel, followed by water (20 mL) and a saturated $NH_4Cl_{(aq)}$ solution (10 mL). The mixture was stirred at ambient temperature for 30 minutes, then the organic phase was extracted and washed with saturated $NH_4Cl_{(aq)}$ (3 x 30 mL) and water (20 mL) then dried over $MgSO_4$. The solution was filtered and the solvent volume was reduced to 50 mL, before it was added dropwise to a solution of p-toluenesulfonic acid monohydrate (14 g, 74 mmol) in diethyl ether (100 mL). The reaction mixture was stirred at ambient temperature for 12 hours then the resulting biphasic system was slowly added *via* an addition funnel to a solution of Na_2CO_3 (10 g, 94 mmol) in water (100 mL) at 0 °C. The mixture was warmed to room temperature and the organic phase was extracted then washed with $NH_4Cl_{(aq)}$ (2 x 30 mL) and water (30 mL) and dried over $MgSO_4$. The solution was filtered and all volatiles removed *in vacuo.* The crude H[Cp^{Me4Bz}] (mixture of two isomers and unreacted enone) was purified by fractional distillation (5 x 10^{-2} mbar at 54-58 ºC; oil bath 130 ºC) to give the desired compound (6 g, 40%).

H[Cp^{Me4Bz}] (1.0 g, 4.7 mmol) was freeze-thaw degassed then dissolved in THF (10 mL) and to this was added dropwise a solution of K[CH_2Ph] (0.560 g, 4.29 mmol, 0.9 mol equivalents) in THF (25 mL) at 0 °C. The resulting white suspension was warmed to ambient temperature and stirred for 12 hours. The mixture was filtered and the solids washed with THF (2 x 5 mL) and pentane (2 x 10 mL) then dried *in vacuo* to give the title compound (0.630 g, 59%). Characterisation of K[Cp^{Me4Bz}] was not achieved due to its insolubility in most organic solvents.

4.4 General Method for the Preparation of Complexes [U(COT^{TIPS2})(Cp^{R})]: Method A

In a typical procedure, UI_3 was dissolved in THF (150 mL) and to this solution was added a 1 mol equivalent solution/suspension of K[Cp^{R}] in THF (50 mL). The mixture was stirred for 24 hours at ambient temperature to yield a purple or green solution of [$UI_2(Cp^{R})(THF)_n$]. THF was removed under reduced pressure and the complex was extracted in toluene and filtered *via* cannula then dried. The residue was dissolved in THF and to this solution was added dropwise a solution of $K_2[COT^{TIPS2}]$ (0.8 – 0.9 mol equivalents) in THF at -35 °C over 40 minutes. The brown mixture was warmed to ambient temperature and the solvent immediately removed under reduced pressure.

The mixed sandwich complex was extracted in pentane and filtered through Celite filter aid on a porosity 3 glass sinter. The brown solution was reduced in volume and cooled to -35 °C to yield crystals of the title compound (see individual details for complexes **1**, **2** and **4 – 5** below).

4.5 [U(COT^{TIPS2})(Cp^{tBu})(THF)] (1.THF)

Prepared according to method A on a 1.90 mmol scale to furnish green crystals from pentane (0.554 g, 34%). ^{1}H NMR (C_7D_8): δ 5.6 (s, br, 2H, Cp/COT-C*H*), 4.9 (s, br, 2H, Cp/COT-C*H*), 1.5 (s, br, 4H, THF), 0.7 (s, br, 4H, THF), -2.8 (s, br, 6H, ^{i}Pr-C*H*), -4.0 (s, br, 18H, ^{i}Pr-CH_3), -4.1 (s, br, 2H, Cp/COT-C*H*), -5.7 (s, br, 18H, ^{i}Pr-CH_3), -12.8 (s, br, 9H, ^{t}Bu-CH_3), -58.2 (s, br, 2H, Cp/COT-C*H*), -74.8 (s, br, 2H, Cp/COT-C*H*). ^{29}Si{^{1}H} NMR (C_7D_8): δ -134.3 (*Si*^{i}Pr$_3$). Anal. calcd (found) for $C_{39}H_{69}OSi_2U$: C 55.23 (55.20), H 8.20 (7.76). MS (EI): *m/z* = 776 (M^+ - THF).

4.6 [U(COT^{TIPS2})(Cp^{tBu})] (1)

1 was obtained from **1.THF** by drying a solid sample at 10^{-5} mbar at ambient temperature for two hours, or by thoroughly drying a solution of **1.THF** in pentane at ambient temperature. The residue of **1** was dissolved in pentane and filtered through Celite filter aid on a porosity 3 glass sinter then dried *in vacuo* to furnish **1** as a green powder in quantitative yield. Green crystals were obtained by cooling a saturated solution of **1** in pentane to -35 °C. ^{1}H NMR (C_7D_8): δ 10.8 (s, br, 2H, Cp/COT-C*H*), 5.8 (s, br, 2H, Cp/COT-C*H*), 0.0 (s, br, 2H, Cp/COT-C*H*), -4.6 (s, br, 6H, ^{i}Pr-C*H*), -6.8 (s, br, 18H, ^{i}Pr-CH_3), -9.0 (s, br, 18H, ^{i}Pr-CH_3), -17.9 (s, br, 9H, ^{t}Bu-CH_3), -54.7 (s, br, 2H, Cp/COT-C*H*), -76.8 (s, br, 2H, Cp/COT-C*H*). ^{29}Si{^{1}H} NMR (C_7D_8): δ -126.7 (*Si*^{i}Pr$_3$).

4.7 [U(COT^{TIPS2})(Cp^{tBu2})] (2)

Prepared according to method A on a 1.45 mmol scale to furnish green crystals from pentane (0.425 g, 35%). ^{1}H NMR (C_7D_8): δ 20.2 (s, br, 2H, Cp/COT-C*H*), 10.6 (s, br, 1H, Cp-C*H*), -2.6 (s, br, 6H, ^{i}Pr-C*H*), -4.4 (s, br, 18H, ^{i}Pr-CH_3) -6.6 (s, br, 18H, ^{i}Pr-CH_3), -14.7 (s, br, 2H, Cp/COT-C*H*), -17.0 (s, br, 18H, ^{t}Bu-CH_3), -58.1 (s, br, 2H, Cp/COT-C*H*), -90.4 (s, br, 2H, Cp/COT-C*H*). ^{29}Si{^{1}H} NMR (C_7D_8): δ -122.5 (*Si*^{i}Pr$_3$). Anal. calcd (found) for $C_{39}H_{69}Si_2U$: C 55.72 (56.29), H 8.48 (8.36). MS (EI): *m/z* = 831 (M^+).

4.8 [U(COT^{TIPS2})(Cp^{tBu3})] (3)

To a solution of UI_3 (1.44 g, 2.33 mmol) in THF (150 mL) was added a beige suspension of K[Cp^{tBu3}] (0.630 g, 2.32 mmol) in THF (30 mL) at ambient temperature. The mixture was stirred for 24 hours to yield a purple solution of [UI_2(Cp^{tBu3})(THF)$_n$] and pale precipitates. The mixture was cooled to -35 °C and to this was added dropwise a solution of K_2[COT$^{(Si\mathit{i}Pr3)2}$] (0.98 g, 1.98

mmol, 0.85 equivalents) in THF (30 mL) over 40 minutes. The brown mixture was stirred at ambient temperature for 24 hours and the solvent was removed under reduced pressure. The title compound was extracted in pentane and filtered through Celite filter aid on a porosity 3 glass sinter to give a green solution. The solution was concentrated to furnish green crystals at -35 °C (1.34 g, 65%). ^{1}H NMR (C_7D_8): δ 2.8 (s, br, 2H, Cp/COT-C*H*), -3.1 (overlapping, br, 24H, ^{i}Pr-CH_3, ^{i}Pr-C*H*), -4.7 (overlapped, br, 20H, ^{i}Pr-CH_3, Cp/COT-C*H*), -7.8 (s, br, 18H, ^{t}Bu-CH_3), -24.3 (s, br, 9H, ^{t}Bu-CH_3), -50.4 (s, br, 2H, Cp/COT-C*H*), -76.1 (s, br, 2H, Cp/COT-C*H*). ^{29}Si{^{1}H} NMR (C_7D_8): δ -116.6 (*Si*^{i}Pr$_3$). Anal. calcd (found) for $C_{43}H_{77}Si_2U$: C 58.14 (57.95), H 8.74 (8.81). MS (EI): *m/z* = 888 (M^+).

4.9 [U(COT^{TIPS2})(Cp^{TIPS2})] (4)

Prepared according to method A on a 1.70 mmol scale to furnish green crystals from pentane (0.848 g, 52%). ^{1}H NMR (C_7D_8, 373 K): δ 19.0 (s, br, 2H, Cp/COT-C*H*), 8.1 (s, br, unassigned), 7.7 (s, br, unassigned), -1.6 (s, br, 6H, ^{i}Pr-C*H*), -2.0 (s, br, 18H, ^{i}Pr-CH_3), -3.3 (s, br, 18H, ^{i}Pr-CH_3), -4.0 (s, br, 18H, ^{i}Pr-CH_3), -4.2 (s, br, 18H, ^{i}Pr-CH_3), -5.8 (s, br, 6H, ^{i}Pr-C*H*), -46.5 (s, br, 2H, Cp/COT-C*H*), -72.8 (s, br, 2H, Cp/COT-C*H*). ^{29}Si{^{1}H} NMR (C_7D_8, 373 K): δ -96.8 (*Si*^{i}Pr$_3$). Anal. calcd (found) for $C_{49}H_{93}Si_4U$: C 56.99 (56.70), H 9.08 (8.69). MS (EI): *m/z* = 1032 (M^+).

NMR studies of 4: The ^{1}H NMR spectrum of **4** at ambient temperature did not show any clearly defined resonances, but variable temperature NMR illustrated fluxional behaviour at this temperature. The COT and Cp ring protons resolve into nine separate resonances below 5 °C indicating C_1 symmetry, and resolve into five proton environments above 35 °C, indicating free movement of the rings on the timescale of the experiment and Cs symmetry.

4.10 [U(COT^{TIPS2})(Cp^{Me4Bz})] (5)

Prepared according to method A on a 1.62 mmol scale. The procedure was modified by carrying out the addition of K_2[COT$^{(SiiPr3)2}$] to [UI_2(Cp^{Me4Bz})(THF)$_n$] at -50 °C over 90 minutes then slowly warming the mixture to ambient temperature and stirring for 12 hours. Green-brown crystals were furnished from a 1:1 mixture of pentane and $SiMe_4$ (0.550 g, 49%). ^{1}H NMR (C_7D_8): δ 41.7 (s, br, 2H, COT-C*H*), 6.6 (s, br, 1H, Ph-C*H*), 6.4 (s, br, 1H, Ph-C*H*), -0.3 (s, br, 6H, Cp-CH_3), -3.1 (s, br, 18H, ^{i}Pr-CH_3), -5.45 (s, br, 2H, CH_2Ph), -6.96 (s, br, 18H, ^{i}Pr-CH_3), -11.0 and -11.3 (two overlapping s, br, 6H, ^{i}Pr-C*H*), -17.8 (s, br 6H, Cp-CH_3), -81.6 (s, br, 2H, COT-C*H*), -118.4 (s, br, 2H, COT-C*H*). 2H presumably from the Ph protons are obscured by the solvent residual peaks. ^{29}Si{^{1}H} NMR (C_7D_8): δ -140 (*Si*^{i}Pr$_3$). Anal. calcd (found) for $C_{42}H_{67}Si_2U$: C 58.24 (58.07), H 7.80 (7.66). MS (EI): *m/z* = 865 (M^+).

4.11 [U(COT^{TIPS2})(Ind^{Me6})] (6)

A yellow solution of KInd^{Me6} (0.61 g, 2.50 mmol) in THF (15 ml) was added dropwise over 15 min to a cooled to 0 °C, pre-stirred solution of UI_3 (1.60 g, 2.50 mmol) in THF (100 ml) and the colour of the solution was observed to change from purple to a dark green with the formation of a white precipitate. The solution was stirred overnight, stripped to dryness and the dark green solids extracted with toluene and filtered. The solids were taken up in THF (50 ml) and the dark green solution cooled to – 78 °C, to this a yellow solution of $K_2(C_8H_6\{Si^iPr_3\text{-}1,4\}_2)$ (1.03 g, 2.08 mmol, 0.83 equivalents) in THF (20 ml) was added dropwise over 1 hr 15 min and the solution was stirred for a further 30 min at this temperature. The reaction vessel was then removed from the cold bath and stirred for 2 hrs 30 min. The colour of the solution was observed to have changed to a dark red and a white precipitate was observed about 20 minutes after the vessel was removed from the cold bath. Volatiles were removed *in vacuo* and solids extracted with toluene and the red/brown solution filtered. The solution was stripped to dryness and crystals were furnished from a minimum amount of pentane, to yield the product as dark red crystals (0.445 g, 20%). ^{1}H NMR (C_7D_8): δ 54.0 (s, br, 1H, COT-C*H*), 19.4 (m, br, COT-C*H*), 5.5 (m, br, 6H, Ind-CH_3), 0.4 (s, br 3H, Ind-CH_3), -1.0 (s, 9H, ^{i}Pr-CH_3), -3.6 (s, 9H, ^{i}Pr-CH_3), -5.6 (s, 9H, ^{i}Pr-CH_3), -6.7 (s, 3H, ^{i}Pr-C*H*), -10.6 (s, 9H, ^{i}Pr-CH_3), -15.1 (s, br, 3H, Ind-CH_3), -17.4 (s, br, 3H, Ind-CH_3), -19.3 (s, 9H, ^{i}Pr-CH_3), -28.0 (s, br, 3H, Ind-CH_3), -50.9 (s, br, 1H, COT-C*H*), -94.1 (s, br, 1H, COT-C*H*), -103.6 (s, br, 1H, COT-C*H*), -117.06 (s, br, 1H, COT-CH). ^{29}Si{^{1}H} NMR (C_7D_8): δ -110.8 (*Si*^{i}Pr$_3$), -138.1 (*Si*^{i}Pr$_3$). Anal. calcd (found) for $C_{41}H_{67}Si_2U$: C 57.50 (57.57), H 7.71 (7.77). MS (EI): *m/z* = 853 (M^+).

4.12 [U(COT^{TIPS2})(Ind^{Me7})] (7)

A yellow suspension of KInd^{Me7} (0.49 g, 1.94 mmol) in THF (15 ml) at –90 °C was added dropwise over 45 min to the pre-stirred solution of UI_3 (1.20 g, 1.94 mmol) in THF (100 ml) at 0 °C and the colour of the solution was observed to change from purple to a dark green with the formation of a white precipitate. The solution was stirred overnight, stripped to dryness and the dark green solids extracted with toluene and filtered. The solids were taken up in THF (50 ml) and the dark green solution cooled to –78 °C, to this a yellow solution of $K_2(C_8H_6\{Si^iPr_3\text{-}1,4\}_2)$ (0.78 g, 1.57 mmol, 0.81 equivalents) in THF (30 ml) was added dropwise over 1 hr and the solution was stirred for a further hour at this temperature. The reaction vessel was then removed from the cold bath and stirred for 1 hr 15 min. The colour of the solution was observed to have changed to a dark red and a white precipitate was observed about 20 minutes after the vessel was removed from the cold bath. Volatiles were removed *in vacuo* and the sticky red/brown solids extracted with pentane, sonicated and filtered on a frit through dry Celite® and crystals were furnished from a minimum pentane to yield the product as dark red crystals (0.405 g, 24%). ^{1}H NMR (C_7D_8): δ 42.6 (s, br, 2H, COT-C*H*),

5.2 (s, br, 6H, Ind-CH_3), 0.6 (s, br, 3H, Ind-CH_3), 0.0 (s, br, 6H, Ind-CH_3), -2.7 (s, 18H, ^{i}Pr-CH_3), -6.0 (s, 18H, ^{i}Pr-CH_3), -16.8 (s, br, 6H, Ind-CH_3), -22.8 (s, 6H, ^{i}Pr-CH), -76.4 (s, br, 2H, COT-CH), -114.1 (s, br, 2H, COT-CH). ^{29}Si{^{1}H} NMR (C_7D_8): δ -122.2 ($Si^{i}Pr_3$). Anal. calcd (found) for $C_{42}H_{69}Si_2U$: C 58.13 (58.12), H 6.46 (6.49). MS (EI): *m/z* = 867 (M^+).

4.13 [U(COT^{TIPS2})(Cp^{tBu})]$_2$(μ-O) (8)

A solution of **1.THF** (90.6 mg, 0.107 mmol) in toluene (5 mL) was cooled to -78 °C and degassed. To this was added 3 equivalents N_2O and the mixture was warmed to ambient temperature over one hour. The mixture was stirred for 24 hours then all volatiles were removed in vacuo. Crystals of **8** suitable for X-ray analysis were grown by slow cooling a pentane solution to -35 °C (37.9 mg, 45%). ^{1}H NMR (C_6D_6): δ 115.6 (s, br, 2H, Cp/COT-CH), 2.1 (br), -0.4 (m, br, 18H, ^{i}Pr-CH_3), -0.5 (m, br, 18H, ^{i}Pr-CH_3), -1.39 (br), -5.0 (br), -10.6 (s, br, 9H, ^{t}Bu-CH_3). ^{29}Si{^{1}H} NMR (C_6D_6): δ -85.7 ($Si^{i}Pr_3$). Anal. calc (found) for $C_{70}H_{122}OSi_4U_2$: C 53.62 (52.44), H 7.84 (7.51)%.

NMR studies: The formation of **8** was reproducibly observed to be the only uranium-containing product by NMR studies of the reaction of **1** or **1.THF** with 1-3 equivalents of N_2O added *via* the Toepler line at - 78 °C.

The formation of **8** from the reaction of **1** or **1.THF** with 0.5-3.5 equivalents of ^{13}CO added *via* the Toepler line at - 78 °C was not observed by NMR within three weeks. **8** crystallised from the reaction mixture after this time but was never observed in solution. NMR studies of the isolated crystals confirmed the formulation.

4.14 [U(COT^{TIPS2})(Ind^{Me6})]$_2$(C_4O_4) (9)

A solution of **6** (100 mg, 0.12 mmol) in toluene (15 mL) was cooled to -78 °C and degassed. To this was added CO (5 psi) and the mixture was warmed to ambient temperature over four hours. The mixture was stirred for 20 minutes then all volatiles were removed in vacuo. Crystals of **9** suitable for X-ray analysis were grown by slow cooling to -50 °C of a pentane solution over several weeks, however, there was insufficient material for further characterisation.

NMR studies: The formation of **9** was reproducibly observed to be the only uranium-containing product by NMR studies of the reaction of **6** with 0.5-5 equivalents of ^{13}CO added *via* the Toepler line at - 78 °C. ^{13}C{^{1}H} NMR (C_7D_8): δ 186 (s, ^{13}CO), -63.5 (m, br, ^{13}C-C_4O_4).

The formation of **9** as one of 2 uranium-containing products was reproducibly observed by NMR studies of the reaction of **6** with 0.5-5 equivalents of ^{13}CO added *via* the Toepler line at - 78 °C.

$^{13}C\{^{1}H\}$ NMR (C_7D_8): δ 272.3 (m, br, ^{13}C-C_3O_3), -63.5 (m, br, ^{13}C-C_4O_4). $^{29}Si\{^{1}H\}$ NMR (C_7D_8): δ -78.8, -79.1, -86.71.

4.15 [U(COT^{TIPS2})(Ind^{Me7})(CO)] (10)

A red solution of **7** (30 mg, 0.035 mmol) in C_7D_8 (0.5 ml) was cooled to -78 °C, degassed and ^{13}CO (*ca.* 2 equivalents) was added *via* the Toepler line. After addition of the gas the tube was warmed to room temperature overnight. The colour of the solution was observed to darken to brown. ^{1}H NMR (C_7D_8): δ 27.51 (v. br, s, 2H, COT ring-C*H*), 4.89 (br, s, 6H, Ind-C*H*$_3$), -0.64 (br, s, 6H, ^{i}Pr-C*H*), -2.10 (br, s, 3H, Ind-C*H*$_3$), -2.65 (s, 18H, ^{i}Pr-C*H*$_3$), -5.39 (s, 18H, ^{i}Pr-C*H*$_3$), -14.37 (br, s, 6H, Ind-C*H*$_3$), -20.62 (br, s, 6H, Ind-C*H*$_3$), -69.59 (v. br, s, 2H, COT ring-C*H*), -97.62 (v. br, s, 2H, COT ring-C*H*). React IR™ Studies: The reaction of **7** with 2.5 equivalents of ^{13}CO at -50 ºC in methylcyclohexane was monitored by *in situ* IR spectroscopy. Initial: ν^{13}_{CO} 1905 cm^{-1}. After addition of excess ^{12}CO and stirring at ambient temperature for 12 hr: ν^{12}_{CO} 1945 cm^{-1}.

4.16 [U(COT^{TIPS2})(Ind^{Me7})](μ-C_2O_2) (11)

After exposure of **7** to an atmosphere of ^{13}CO for at least 7 days: $^{13}C\{^{1}H\}$ NMR (C_7D_8): δ 395 (s, ^{13}C-C_2O_2). ^{1}H NMR (C_7D_8): δ 25.81 (br, s, 6H, Ind-C*H*$_3$), 14.51 (br, s, 6H, Ind-C*H*$_3$), 2.40 (s, 6H, Ind-C*H*$_3$), 2.20 (s, 6H, Ind-C*H*$_3$), 1.82 (s, 6H, Ind-C*H*$_3$), -3.53 (s, 18H, ^{i}Pr-C*H*$_3$), -3.86 (s, 6H, Ind-C*H*$_3$), -8.38 (s, 18H, ^{i}Pr-C*H*$_3$), -13.08 (br, s, 6H, ^{i}Pr-C*H*), -18.44 (br, s, 3H, Ind-C*H*$_3$), -45.24 (v. br, s, 2H, COT ring-C*H*), -53.40 (v. br, s, 2H, COT ring-C*H*), -81.70 (v. br, s, 2H, COT ring-C*H*).

4.17 [U(COT^{TIPS2})(Cp^{tBu})]$_2$(CO_3) (12)

To a degassed solution of **1** (85.0 mg, 1.09 x 10^{-4} mol) in toluene was added three equivalents of CO_2 at -78 °C. Warming the mixture resulted in the formation of a red/brown solution over several minutes. Removal of all volatiles and extraction of the title compound in pentane furnished a red solution which yielded crystals at -35 °C. (39.9 mg, 45%). ^{1}H NMR (C_6D_6): δ 33.7 (s, br, 2H, Cp/COT-C*H*), 9.7 (s, br, 2H, Cp/COT-C*H*), -4.8 (d, $^{3}J_{HH}$ = 6.8 Hz, 18H, ^{i}Pr-C*H*$_3$), -6.4 (d, $^{3}J_{HH}$ = 6.6 Hz, 18H, ^{i}Pr-C*H*$_3$), -8.3 (s, br, 6H, ^{i}Pr-C*H*),-13.3 (s, br, 9H, ^{t}Bu-C*H*$_3$), -15.7 (s, br, 2H, Cp/COT-C*H*), -21.7 (s, br, 2H, Cp/COT-C*H*), -44.7 (s, br, 2H, Cp/COT-C*H*). $^{13}C\{^{1}H\}$ NMR (C_6D_6): δ 195.4 (br, $w_{½}$ = 375 Hz, *C*O_3). $^{29}Si\{^{1}H\}$ NMR (C_6D_6): δ -100.8 (*Si*^{i}Pr$_3$). Anal. calcd (found) for $C_{71}H_{122}O_3Si_4U_2$: C 52.90 (52.44), H 7.63 (7.51). MS (EI): *m/z* = 1613 (M^+).

4.18 [U(COT^{TIPS2})(Cp^{tBu3})]$_2$(μ-O) (13)

The formation of **13** was reproducibly observed to be the only uranium-containing product by NMR studies of the reaction of **3** with 0.5-3 equivalents of $^{13}CO_2$ added *via* the Toepler line at - 78 °C. $^{13}C\{^1H\}$ NMR (C_7D_8): δ 186 (s, ^{13}CO).

Alternative synthesis: To a degassed solution of [U(COT^{TIPS2})(Cp^{tBu3})] (280 mg, 3.15 x 10^{-4} mol) in toluene was added three equivalents of N_2O at -78 °C. Warming the mixture to room temperature resulted in a colour change from olive green to red/brown. **13** was obtained quantitatively by NMR. ^1H NMR (C_7D_8): δ 39.2 (s, br, 2H, Cp/COT-C*H*), 11.7 (s, br, 9H, ^{t}Bu-CH_3), -0.5 (s, br, 18H, ^{i}Pr-CH_3), -2.3 (s, br, 2H, Cp/COT-C*H*), -4.1 (s, br, 18H, ^{i}Pr-CH_3), -5.0 (s, br, 6H, ^{i}Pr-C*H*), -9.5 (s, br, 18H, ^{t}Bu-CH_3), -37.5 (s, br, 2H, Cp/COT-C*H*). $^{29}Si\{^1H\}$ NMR (C_7D_8): δ -73.3 (*Si*^{i}Pr$_3$).

4.19 [U(COT^{TIPS2})(Cp^{TIPS2})]$_2$(μ-O) (14)

The formation of **14** was reproducibly observed to be the only uranium-containing product by NMR studies of the reaction of **3** with 0.5-2 equivalents of $^{13}CO_2$ added *via* the Toepler line at - 78 °C. $^{13}C\{^1H\}$ NMR (C_7D_8): δ 186 (s, ^{13}CO).

Alternative synthesis: To a degassed solution of **4** (226 mg, 2.18 x 10^{-4} mol) in toluene was added three equivalents of N_2O at -78 °C. Warming the mixture to room temperature resulted in a colour change from green to red/brown. **14** was obtained quantitatively by NMR. ^1H NMR (C_7D_8): δ 37.6 (s, br, 2H, Cp/COT-C*H*), 5.2 (s, br, 18H, ^{i}Pr-CH_3), 4.6 (s, br, 6H, ^{i}Pr-C*H*), 4.3 (s, br, 18H, ^{i}Pr-CH_3), -2.1 (s, br, 18H, ^{i}Pr-CH_3), -5.2 (s, br, 18H, ^{i}Pr-CH_3), -6.6 (s, br, 6H, ^{i}Pr-C*H*), -22.9 (s, br, 2H, Cp/COT-C*H*), -38.5 (s, br, 2H, Cp/COT-C*H*), -39.7 (s, br, 2H, Cp/COT-C*H*). $^{29}Si\{^1H\}$ NMR (C_7D_8): δ -40.7 (*Si*^{i}Pr$_3$), -52.6 (*Si*^{i}Pr$_3$).

4.20 [U(COT^{TIPS2})(Ind^{Me6})]$_2$(μ-CO_3) (15)

A red solution of **6** (26 mg, 0.03 mmol) in d_8- toluene was cooled to -78 °C, degassed, and $^{13}CO_2$ (*ca.* 2.3 equivalents) was added *via* the Toepler line. After addition of the gas the tube was warmed to room temperature overnight. The colour of the solution was observed to redden on addition of gas. $^{13}C\{^1H\}$ NMR (C_7D_8): δ 210.5 (^{13}C-CO_3), 209.2 (^{13}C- CO_3), 184.8 (s, ^{13}CO), 123 (s, $^{13}CO_2$), -63.5 (m, br, ^{13}C-C_4O_4). MS (EI): *m/z* = 1814, 1697, 1235, 1098.

4.21 [U(COT^{TIPS2})(Ind^{Me7})]$_2$(μ-CO_3) (16)

A red solution of **7** (32 mg, 0.037 mmol) in d_8- toluene was cooled to -78 °C, degassed and $^{13}CO_2$ (*ca.* 2 equivalents) was added *via* the Toepler line. After addition of the gas the tube was warmed to room temperature overnight. The colour of the solution was observed to redden on addition of gas. $^{13}C\{^1H\}$ NMR (C_7D_8): δ 186 (s, ^{13}CO), 180.8 (^{13}C-CO_3), 123 (s, $^{13}CO_2$).

4.22 X-ray Crystallographic Studies

Data for **1** – **9** and **12** were collected on a Enraf-Nonius KappaCCD diffractometer with graphite-monochromated Mo K α radiation (λ = 0.71073) source at 173 K using an Oxford Cryosystems Cobra low temperature device, operating in ω scanning mode with ψ and ω scans to fill the Ewald sphere. The programs used for control and integration were Collect,[30] Scalepack and Denzo.[31] Absorption corrections were based on equivalent reflections using SADABS.[32] The crystals were mounted on a glass fibre with silicon grease, from dried vacuum oil kept over 4 Å molecular sieves in an MBraun glovebox under Ar. All solutions and refinements were performed using the WinGX or Olex2 packages and software therein. All non-hydrogen atoms were refined with anisotropic atomic displacement parameters (adps) except where disorder was modelled over 2 partially occupied sites and isotropic adps were retained. Hydrogen atoms were included as part of a riding model, Me groups were as a mixture of riding model and rigid rotors to minimise Me H clashes. In **1.THF**, **4**, **5**, **9** and **12** regions of poorly defined solvent were accounted for using SQUEEZE within PLATON. Details are given in the supplementary crystallographic data: CCDC 1506039 (**1**), 1506315 (**1.THF**), 1506313 (**2**), 1439555 (**3**), 1506310 (**4**), 1506309 (**5**), 1506311 (**6**), 1506312 (**7**), 1564238 (**8**), 1506314 (**9**) and 1561910 (**12**).

Crystal data for **1**. Green air sensitive block 0.06 x 0.06 x 0.06 mm^3, $C_{35}H_{62}Si_2U$, a = 12.901(3), b = 11.578(2), c = 24.039(5) Å, α = 90°, β = 90°, γ = 90°, U = 3590.6(12) Å^3, orthorhombic, Pbcm (No. 57), Z = 4, total reflections 38498, independent reflections 4034, R_{int} = 0.0767, θmax = 25.326, R1 [I > 2σ(I)] = 0.0751, wR^2 = 0.1735 and 186 parameters.

Crystal data for **1.THF** Black air sensitive block 0.20 x 0.10 x 0.04 mm^3, $C_{39}H_{69}O_1Si_2U$, a = 22.9509(3), b = 14.9588(2), c = 25.4768(3) Å, α = 90°, β = 100.7030(10)°, γ = 90°, U = 8594.48(19) Å^3, monoclinic, P21/n (No. 14), Z = 8, total reflections 49609, independent reflections 18690, R_{int} = 0.0791, θmax = 27.090, R1 [I > 2σ(I)] = 0.0550, wR^2 = 0.1278 and 768 parameters.

Crystal data for **2** Green air sensitive needle 0.50 x 0.10 x 0.06 mm^3, $C_{39}H_{69}Si_2U$, a = 15.25670(10), b = 27.5882(3), c = 38.2824(5) Å, α = 90°, β = 90°, γ = 90°, U = 16113.3(3) Å^3, orthorhombic, Pbca (No. 61), Z = 16, total reflections 131596, independent reflections 17230, R_{int} = 0.0837, θmax = 27.103, R1 [I > 2σ(I)] = 0.0602, wR^2 = 0.1318 and 797 parameters.

Crystal data for **3** Green air sensitive plate 0.16 x 0.08 x 0.08 mm^3, $C_{43}H_{77}Si_2U$, a = 13.1825(2), b = 15.1917(2), c = 21.8055(4) Å, α = 90°, β = 101.3040(10)°, γ = 90°, U = 4282.16(12) Å^3, monoclinic, P21/n (No. 14), Z = 4, total reflections 68676, independent reflections 9415, R_{int} = 0.1352, θmax = 27.097, R1 [I > 2σ(I)] = 0.0460, wR^2 = 0.0949 and 415 parameters.

Crystal data for **4** Green air sensitive prism 0.14 x 0.10 x 0.08 mm^3, $C_{49}H_{93}Si_4U$, a = 11.7861(2), b = 21.7821(4), c = 24.2194(5) Å, α = 90°, β = 110.4220(10)°, γ = 90°, U = 5826.95(19) $Å^3$, monoclinic, P21/c (No. 14), Z = 4, total reflections 79291, independent reflections 12777, R_{int} = 0.0779, θmax = 27.103, R1 [I > 2σ(I)] = 0.0495, wR^2 = 0.0789 and 511 parameters.

Crystal data for **5** Brown air sensitive plate 0.12 x 0.06 x 0.04 mm^3, $C_{42}H_{67}Si_2U$, a = 13.322(5), b = 15.536(5), c = 21.852(5) Å, α = 78.943(5)°, β = 84.895(5)°, γ = 71.055(5)°, U = 4197(2) $Å^3$, triclinic, P^{-1} (No. 2), Z = 2, total reflections 56173, independent reflections 18990, R_{int} = 0.0752, θmax = 26.371, R1 [I > 2σ(I)] = 0.0440, wR^2 = 0.1042 and 815 parameters.

Crystal data for **6** Black air sensitive needle 0.20 x 0.03 x 0.01 mm^3, $C_{41}H_{67}Si_2U$, a = 15.2508(2), b = 26.5518(5), c = 19.8423(4) Å, α = 90°, β = 96.332(1)°, γ = 90°, U = 7985.8(2) $Å^3$, monoclinic, P21/n (No. 14), Z = 8, total reflections 112708, independent reflections 15662, R_{int} = 0.1844, θmax = 26.009, R1 [I > 2σ(I)] = 0.0620, wR^2 = 0.0889 and 822 parameters.

Crystal data for **7** Black air sensitive plate 0.22 x 0.15 x 0.06 mm^3, $C_{42}H_{69}Si_2U$, a = 15.2615(1), b = 26.6255(3), c = 20.1330(2) Å, α = 90°, β = 96.016(1)°, γ = 90°, U = 8135.89(13) $Å^3$, monoclinic, P21/n (No. 14), Z = 8, total reflections 113101, independent reflections 18524, R_{int} = 0.0868, θmax = 27.102, R1 [I > 2σ(I)] = 0.0450, wR^2 = 0.0796 and 822 parameters.

Crystal data for **8** Red air sensitive plate 0.24 x 0.16 x 0.06 mm^3, $C_{70}H_{122}OSi_4U_2$, a = 8.8559(2), b = 15.4195(5), c = 27.5491(7) Å, α = 91.252(2)°, β = 91.929(2)°, γ = 106.109(3)°, U = 3610.26(18) $Å^3$, triclinic, P^{-1} (No. 2), Z = 2, total reflections 44741, independent reflections 14012, R_{int} = 0.0641, θmax = 67.074, R1 [I > 2σ(I)] = 0.0456, wR^2 = 0.1359 and 724 parameters.

Crystal data for **9** Red air sensitive prism 0.25 x 0.10 x 0.05 mm^3, $C_{86}H_{132}O_4Si_4U_2$, a = 25.7129(11) b = 20.1749(9), c = 12.0421(4) Å, α = 90°, β = 116.292(2)°, γ = 90°, U = 5600.6(4) $Å^3$, monoclinic, C2/m (No. 12), Z = 2, total reflections 33000, independent reflections 5653, R_{int} = 0.0748, θmax = 26.035, R1 [I > 2σ(I)] = 0.0344, wR^2 = 0.0709 and 228 parameters.

Crystal data for **12** Red air sensitive prism 0.14 x 0.12 x 0.04 mm^3, $C_{71}H_{122}O_3Si_4U_2$, a = 24.9079(2) b = 13.5457(2), c = 25.5597(3) Å, α = 90°, β = 113.46°, γ = 90°, U = 7910.56(16) $Å^3$, monoclinic, P21/n (No. 14), Z = 8, total reflections 93022, independent reflections 13391, R_{int} = 0.0947, θmax = 24.701, R1 [I > 2σ(I)] = 0.0624, wR^2 = 0.1496 and 721 parameters.

Acknowledgements

We thank the European Research Council (F.G.N.C), the EPSRC (J.H.F), and the Ivor Nixon Fund (R.J.K) for financial support. We thank Dr Iain J. Day for assistance with NMR spectroscopy and

Dr Alaa Abdul-Sada for mass spectrometry (University of Sussex). We also thank Prof. D. O'Hare for the kind donation of $HInd^{Me7}$ (Oxford University).

References

(1) (a) M. B. Jones, A. J. Gaunt, Chem. Rev. 113 (2013) 1137. (b) S. T. Liddle, Angew. Chem. Int. Ed. 54 (2015) 8604. (c) T. W. Hayton, Dalton Trans. 39 (2010) 1145. (d) T. W. Hayton, Chem. Commun. 49 (2013) 2956.
(2) W. J. Evans, Organometallics, 35 (2016) 3088.
(3) M. R. MacDonald, M. E. Fieser, J. E. Bates, J. W. Ziller, F. Furche, W. J. Evans J. Am. Chem. Soc., 135 (2013) 13310.
(4) C. J. Windorff, G. P. Chen, J. N. Cross, W. J. Evans, F. Furche, A. J. Gaunt, M. T. Janicke, S. A. Kozimor, B. L. Scott J. Am. Chem. Soc., 135 (2017) 3970.
(5) D. S. La Pierre, A. Scheurer, F. W. Heinemann, W. Hieringer, K. Meyer, Angew. Chem. Int. Ed., 53 (2014) 7158.
(6) (a) P. L. Arnold, Chem. Commun. 47 (2011) 9005. (b) I. Castro-Rodríguez, K. Meyer, Chem. Commun. (2006) 1353. (c) O. P. Lam, C. Anthon, K. Meyer, Dalton Trans. (2009) 9677. (d) A. R. Fox, S. C. Bart, K. Meyer, C. C. Cummins, Nature. 455 (2008) 341. (e) P. L. Arnold, Z. R. Turner, Nature Rev. 1 (2017) 0002. (f) H. S. La Pierre, K. Meyer, Prog. Inorg. Chem. 58 (2014) 303. (g) B. M. Gardner, S. T. Liddle, Eur. J. Inorg. Chem. (2013) 3753.
(7) I. Castro-Rodriguez, K. Meyer, J. Am. Chem. Soc.,127 (2005) 11242–11243.
(8) W. J. Evans, S. A. Kozimor, J. W. Ziller, J. Am. Chem. Soc. 125 (2003) 14264.
(9) P. Roussel, P. Scott, J. Am. Chem. Soc. 120 (1998) 1070.
(10) D. M. King, F. Tuna, E. J. L. McInnes, J. McMaster, W. Lewis, A. J. Blake, S. T. Liddle, Science, 337 (2012) 717.
(11) O. T. Summerscales, F. G. N. Cloke, P. B. Hitchcock, J. C. Green, N. Hazari, Science 311 (2006) 829. (b) O. T. Summerscales, F. G. N. Cloke, P. B. Hitchcock, J. C. Green, N. Hazari, J. Am. Chem. Soc. 128 (2006) 9602. (c) N. Tsoureas, O. T. Summerscales, F. G. N. Cloke, S. M. Roe, Organometallics 32 (2013) 1353. (d) A. S. P. Frey, F. G. N. Cloke, P. B. Hitchcock, I. J. Day, J. C. Green, G. Aitken, J. Am. Chem. Soc. 130 (2008) 13816.
(12) (a) O. T. Summerscales, A. S. P. Frey, F. G. N. Cloke, P. B. Hitchcock, Chem. Commun. (2009) 198. (b) N. Tsoureas, L. Castro, A. F. R. Kilpatrick, F. G. N. Cloke, L. Maron, Chem. Sci. 5 (2014) 3777. (c) C. J. Inman, A. S. P. Frey, A. F. R. Kilpatrick, F. G. N. Cloke, S. M. Roe, Organometallics DOI 10.1021/acs.organomet.7b00263.
(13) (a) C. E. Kefalidis, A. S. P. Frey, S. M. Roe, F. G. N. Cloke, L. Maron, Dalton Trans., 43 (2014) 11202. (b) A. S. P. Frey, F. G. N. Cloke, M. P. Coles, L. Maron, T. Davin, Angew. Chem. Int. Ed. 50 (2011) 6881.
(14) (a) R. J. Kahan, F. G. N Cloke, S. M. Roe, F. Nief, New J. Chem. (2015) 7602. (b) J. H. Farnaby, F. G. N. Cloke, M. P. Coles, J. C. Green, G. Aitken, Comptes Rendus Chimie, 13 (2010) 812.
(15) I. A. Guzei, M. Wendt, Dalton Trans. (2006) 3991.
(16) K. Wen, J. Zhongsheng, C. Wenqi, J. Chem. Soc., Chem. Comm. 10 (1991) 680.
(17) (a) P. G. Laubereau, L. Ganguly, J. H. Burns, B. M. Benjamin, J. L. Atwood, J. Selbin, Inorg. Chem. 10 (1971) 2274. (b) J. H. Burns, P. G. Laubereau, Inorg. Chem. 12 (1971) 2789. (c) J. Meunier-Piret,J. P. Declercq, G. Germain, M. Van Meerssche, Bull. Chim. Soc. Bel. 89 (1980) 121. (d) J. Meunier-Piret M. Van Meerssche, Bull. Soc. Chim. Belg. 93 (1984) 299.

(18) (a) M. del Mar Conejo, J. S. Parry, E. Carmona, M. Schultz, J. G. Brennan, S. M. Beshouri, R. A. Andersen, R. D. Rogers, S. Coles, M. B. Hursthouse, Chem. Eur. J. 5 (1999) 3000. (b) J. G. Brennan, R. A. Andersen, J. L. Robbins, J. Am. Chem. Soc. 108 (1986) 335. (c) J. S. Parry, E. Carmona, S. Coles, M. B. Hursthouse, J. Am. Chem. Soc. 117 (1995) 2649. (d) W. J. Evans, S. A. Kozimor, G. W. Nyce, J. W. Ziller, J. Am. Chem. Soc. 125 (2003) 13831.
(19) (a) G. Aitken, N. Hazari, A. S. P. Frey, F. G. N. Cloke, O. T. Summerscales, J. C. Green, Dalton Trans. 40 (2011) 11080. (b) D. McKay, A. S. P. Frey, J. C. Green, F. G. N. Cloke, L. Maron, Chem. Commun, 48 (2012) 4118.
(20) (a) P. L. Arnold, Z. R. Turner, R. M. Bellabarba, R. P. Tooze, Chem. Sci., 2 (2011) 77. (b) B. M. Gardner, J. C. Stewart, A. L. Davis, J. McMaster, W. Lewis, A. J. Blake, S. T. Liddle, Proc. Natl. Acad. Sci. 109 (2012) 9265. (c) S. M. Mansell, N. Kaltsoyannis, P. L. Arnold, J. Am. Chem. Soc., 133 (2011) 9036.
(21) S. Liu, J. Chem. Phys. 126 (2007) 244103.
(22) Selected examples (a) S. Siek, N. A. Dixon, M. Kumar, J. S. Kraus, K. R. Wells, B. W. Rowe, S. P. Kelley, M. Zeller, G. P. A. Yap, E. T. Papish, Eur. J. Inorg. Chem. (2016) 2495. (b) C. A. P. Goodwin, K. C. Joslin, S. J. Lockyer, A. Formanuik, G. A. Morris, F. Ortu, I. J. Vitorica-Yrezabal, D. P. Mills, Organometallics 34 (2015) 2314. (c) R. M. Mampa, M. A. Fernandes, L. Carlon, Organometallics 33 (2014) 3283.
(23) (a) G. K. Fukin, I. A. Guzei, E. V. Baranov, J. Coord. Chem. 60 (2007) 937. (b) G. K. Fukin, I. A. Guzei, E. V. Baranov, J. Coord. Chem. 61 (2008) 1678. (c) G. G. Skvortsov, D. M. Lyubov, M. V. Yakovenko, G. K. Fukin, A. V. Cherkasov, A. A. Trifonov, Russ. Chem. Bull. Int. Ed. 58 (2009) 1126. (d) G. G. Skvortsov, M. V. Yakovenko, G. K. Fukin, A. V. Cherkasov, A. A. Trifonov, Russ. Chem. Bull. Int. Ed. 56 (2007) 1742.
(24) R. S. Dickson, B. J. Dobney, F. W. Eastwood, J. Chem. Educ. 64 (1987) 898.
(25) F. G. N. Cloke, P. B. Hitchcock, J. Am. Chem. Soc. 124 (2002) 9352.
(26) E. V. Dehmlow, C. Bollmann, Z. Naturforsch B 48b (1993) 457.
(27) P. J. Bailey, R. A. Coxall, C. M. Dick, S. Fabre, L.C. Henderson, C. Herber, S. T. Liddle, D. Loroño-González, A. Parkin, S. Parson, Chem. Eur. J. 9 (2003) 4820.
(28) N. C. Burton, F. G. N. Cloke, P. B. Hitchcock, H. de Lemos and A. A. Sameh, J. Chem. Soc. Chem. Commun. (1989) 1462.
(29) M. J. Harvey, T. P. Hanusa, V. G. Young Jr., J. Organomet. Chem. 626 (2001) 43.
(30) Collect, Bruker-AXS, Madison, WI, 1997–2004.
(31) Otwinowski, Z., Minor, W., Methods Enzymol. 276 (1997) 307.
(32) Sheldrick, G. M.; SADABS V2008/1, University of Göttingen, Göttingen, Germany.